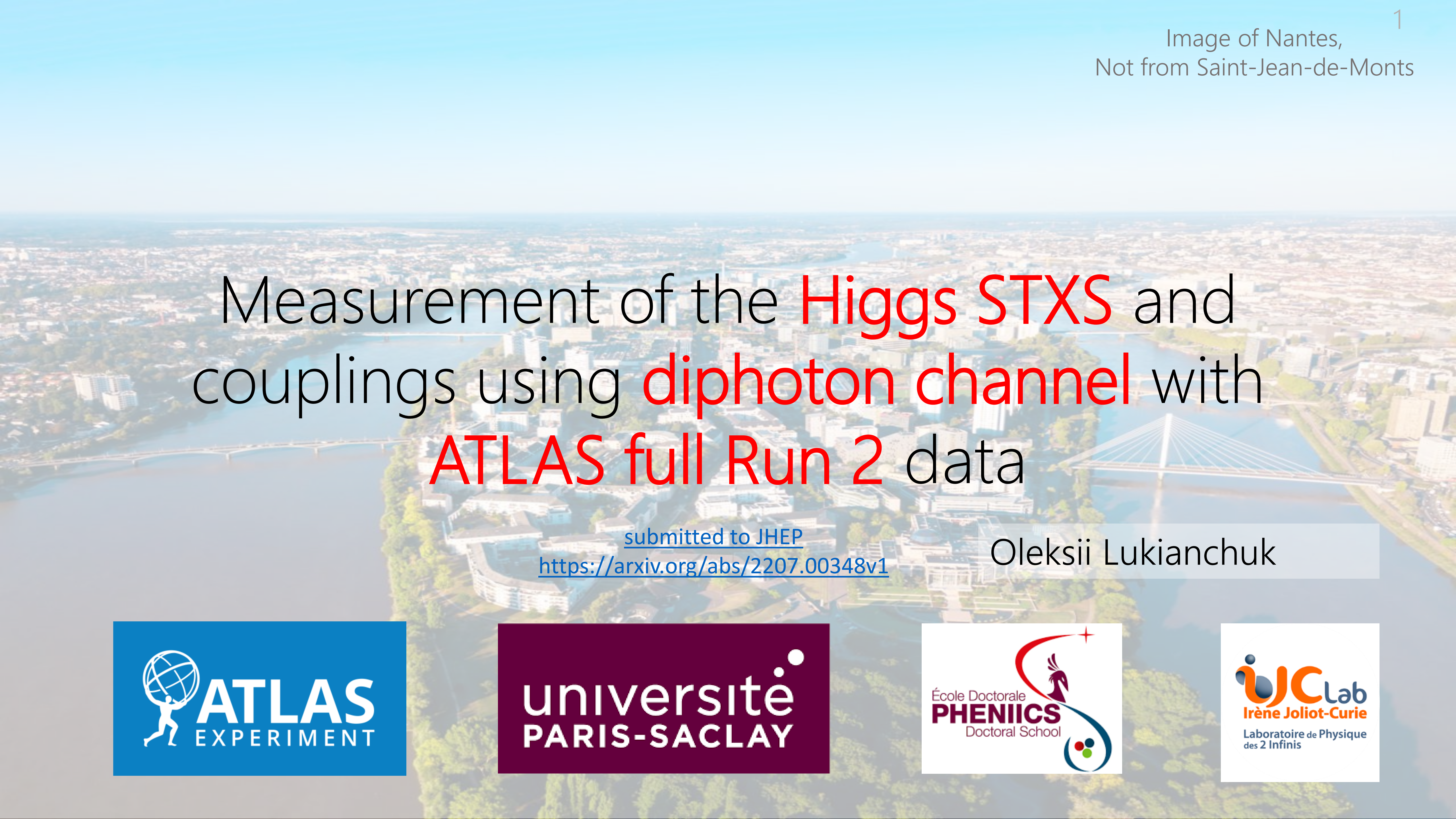

Image of Nantes,
Not from Saint-Jean-de-Monts

Measurement of the Higgs STXS and couplings using diphoton channel with ATLAS full Run 2 data

submitted to JHEP
https://arxiv.org/abs/2207.00348v1

Oleksii Lukianchuk

Introduction

Higgs physics

- Scalar boson **discovered** in **2012** (ATLAS+CMS), **compatible** with **SM Higgs** prediction
- **Coupling** to particles **depends** only **on** their **mass**
- **Any new particle** will **modify** Higgs **production** and **decay** rates

Phys. Lett. B716 (2012) 1-29
Phys. Lett. B 716 (2012) 30

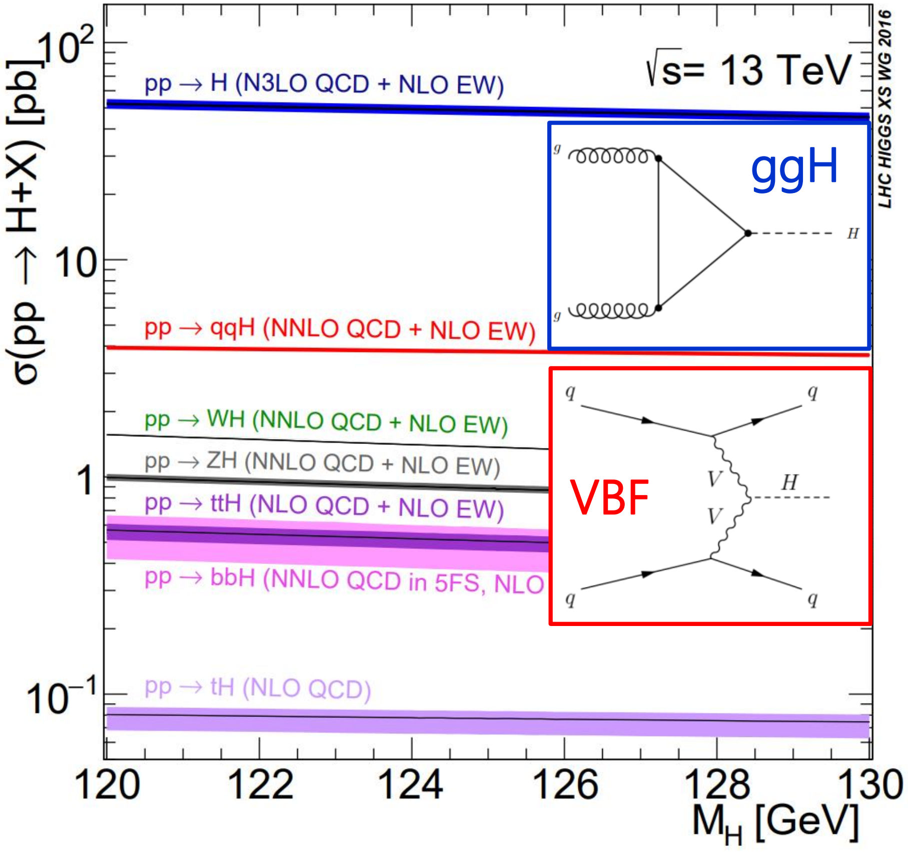

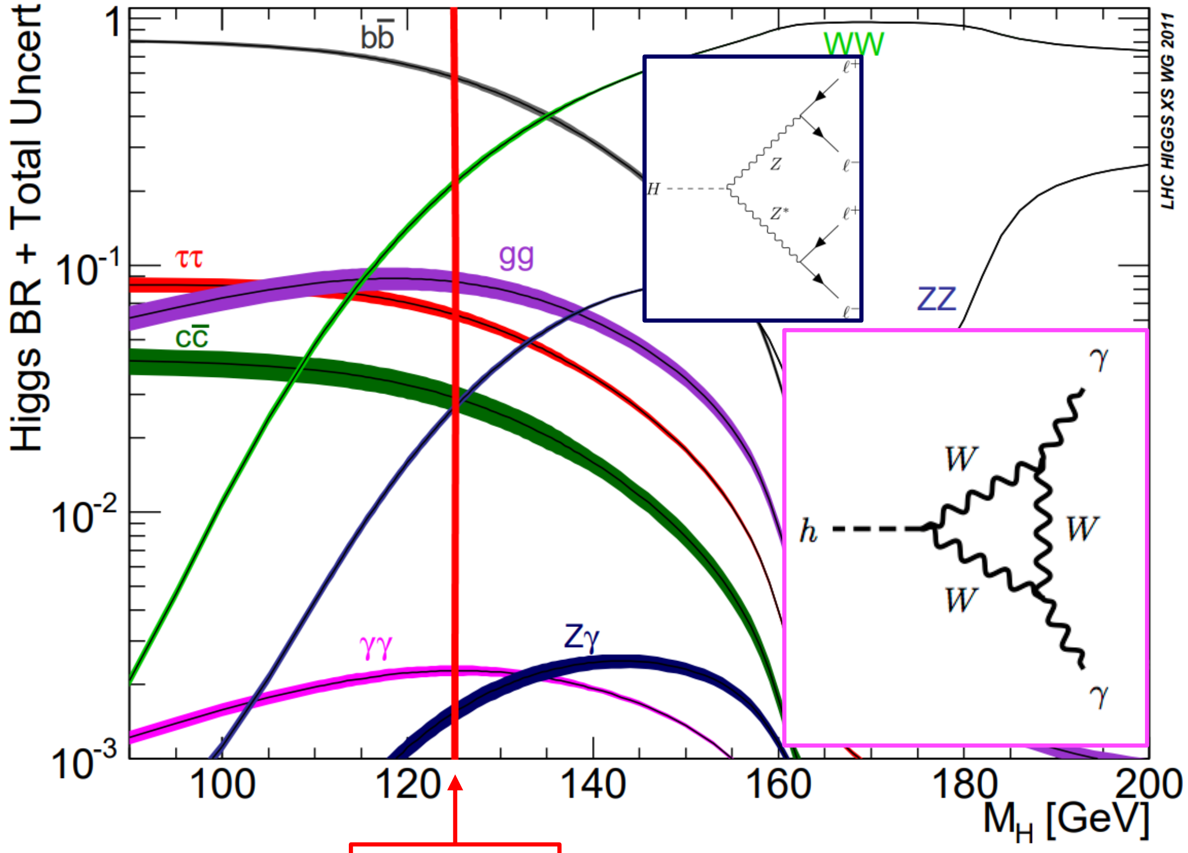

125 GeV

$H \longrightarrow \gamma\gamma$ channel

- Small branching ratio $\mathcal{B}$ (0.228%)
- Clean signature and smooth background

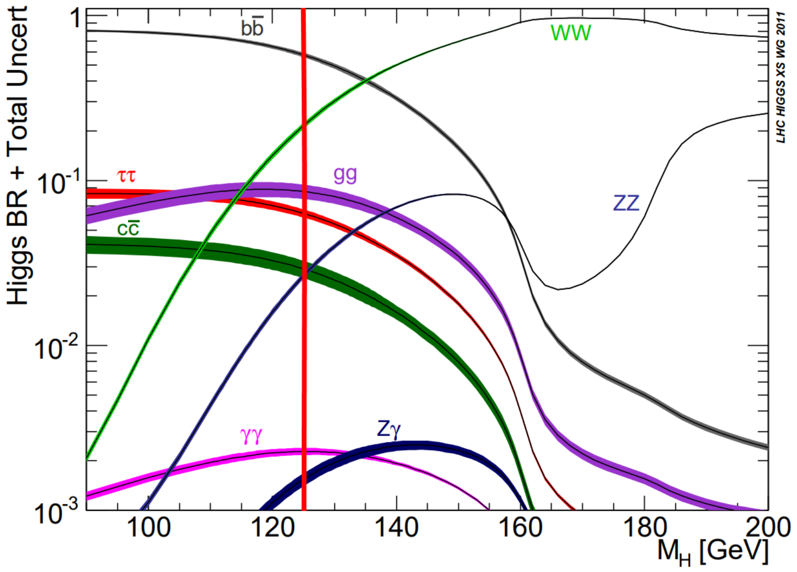

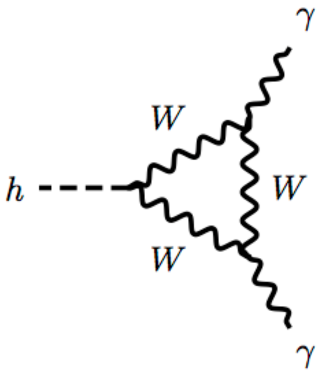

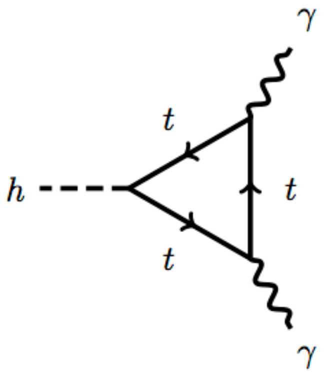

- Current precision on the cross-section O(10%): (full Run2 data: 139 fb^{-1})

$$\left(\sigma \times \mathcal{B}_{\gamma\gamma}\right)_{obs} = 121^{+10}_{-9}\ fb = 121 \pm 7(stat.)\ ^{+7}_{-6}(syst.)\ fb,$$

Probing Phase Space deeper: Simplified Template XS (**STXS**)

Measure production cross-sections in kinematic regions (**truth bins**):

production mode, momentum, #jets, …

Do not include Higgs final state in the description

Use kinematics of other particles

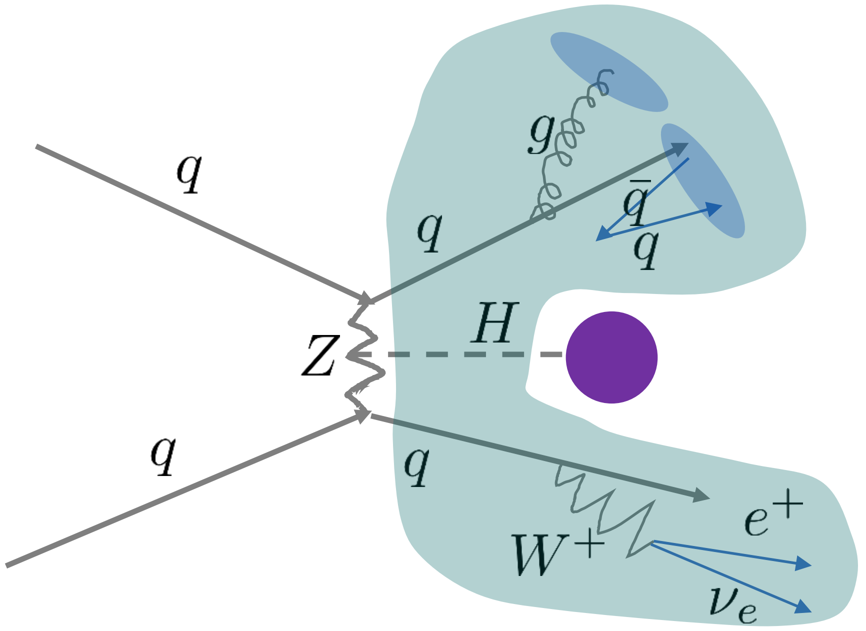

Probing Phase Space deeper: Simplified Template XS (**STXS**)

Measure production cross-sections in kinematic regions (**truth bins**):

production mode, momentum, #jets, …

Advantage:

- **No dependency** on the **final state**

Do **not include Higgs final state** in the description
Use **kinematics** of **other particles**

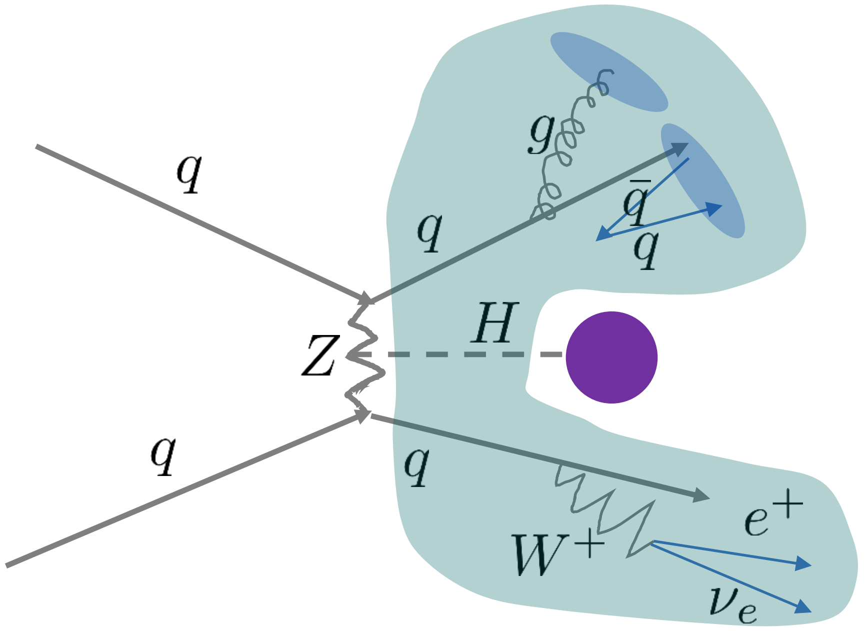

Probing Phase Space deeper: Simplified Template XS (**STXS**)

Measure production cross-sections in kinematic regions (**truth bins**):

production mode, momentum, #jets, …

Advantage:

- **No dependency** on the **final state**
- **No extrapolation** to full **phase-space** (acceptance, kinematical cuts)

Do **not include Higgs final state** in the description
Use **kinematics** of **other particles**

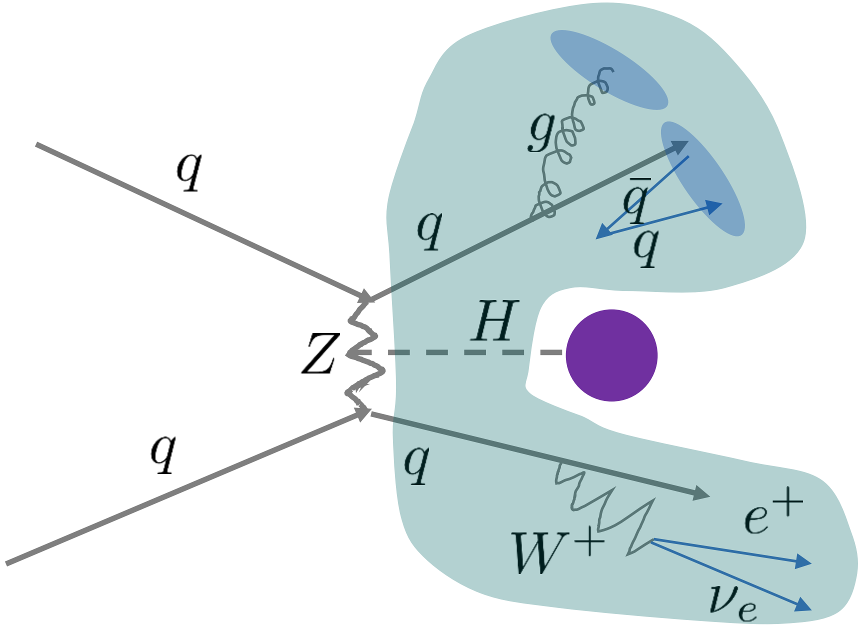

Probing Phase Space deeper: Simplified Template XS (**STXS**)

Measure production cross-sections in kinematic regions (**truth bins**):

production mode, momentum, #jets, …

Advantage:

- **No dependency** on the **final state**
- **No extrapolation** to full **phase-space** (acceptance, kinematical cuts)
- **Easy to combine** (no final state dependency)

Do **not include Higgs final state** in the description
Use **kinematics** of **other particles**

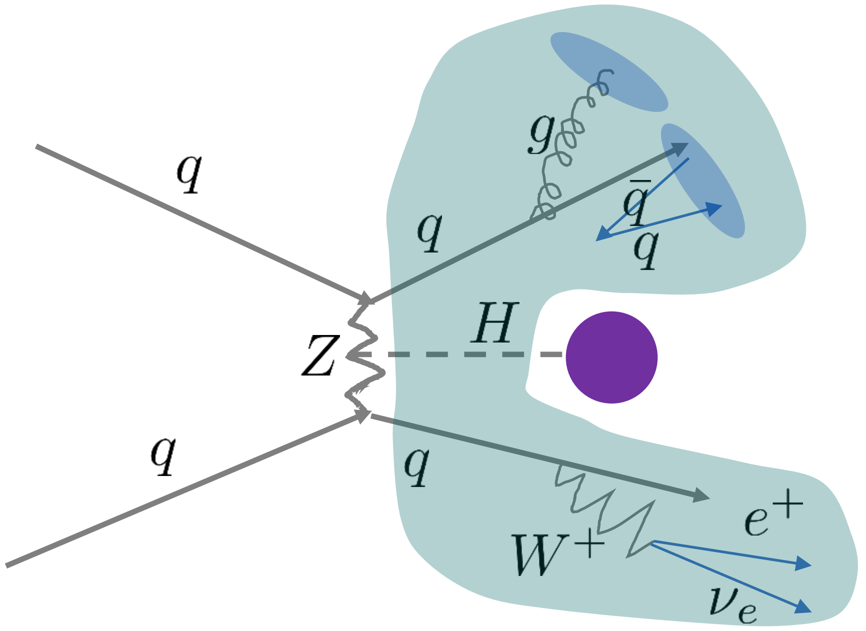

Probing Phase Space deeper: Simplified Template XS (**STXS**)

Measure production cross-sections in kinematic regions (**truth bins**):

production mode, momentum, #jets, …

Advantage:

- **No dependency** on the **final state**
- **No extrapolation** to full **phase-space** (acceptance, kinematical cuts)
- **Easy to combine** (no final state dependency)
- **Reduced theoretical uncertainty** (no dependency on predictions)

Do **not include Higgs final state** in the description

Use **kinematics** of **other particles**

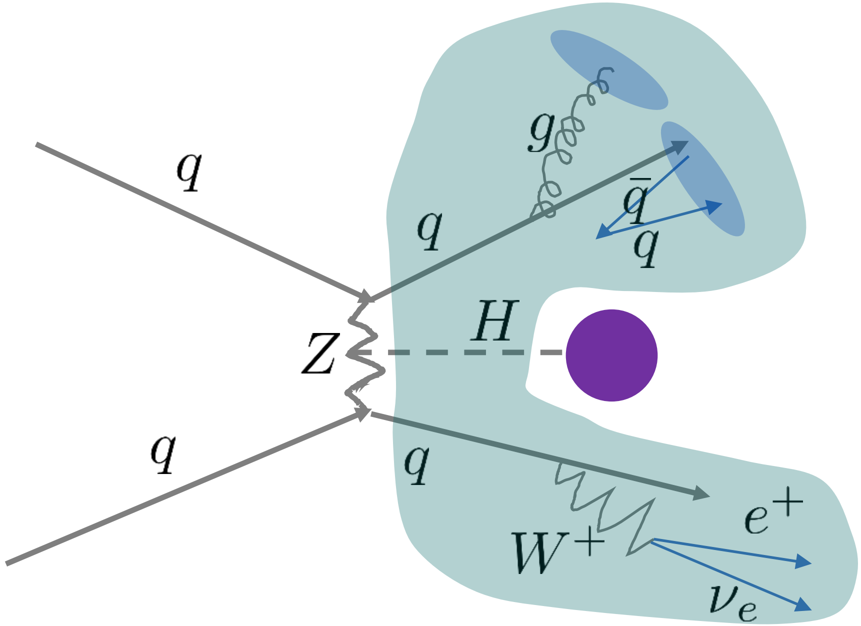

Probing Phase Space deeper: Simplified Template XS (**STXS**)

Measure production cross-sections in kinematic regions (**truth bins**):

production mode, momentum, #jets, …

Advantage:

- **No dependency** on the **final state**
- **No extrapolation** to full **phase-space** (acceptance, kinematical cuts)
- **Easy to combine** (no final state dependency)
- **Reduced theoretical uncertainty** (no dependency on predictions)
- **Enhanced sensitivity to BSM regions (splitting high- and low-pT regions)**

Do **not include Higgs final state** in the description
Use **kinematics** of **other particles**

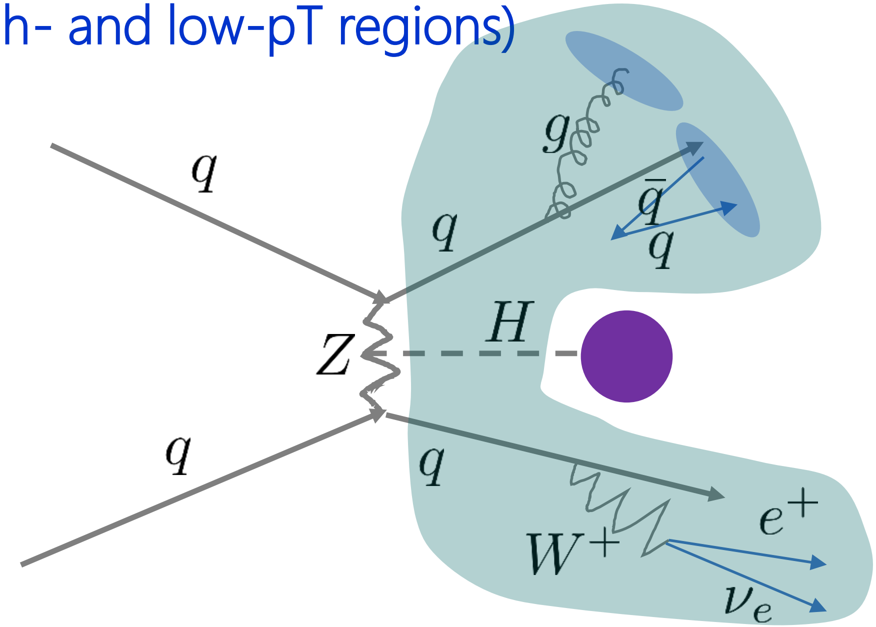

Truth bins in STXS stage 1.2 (merged)

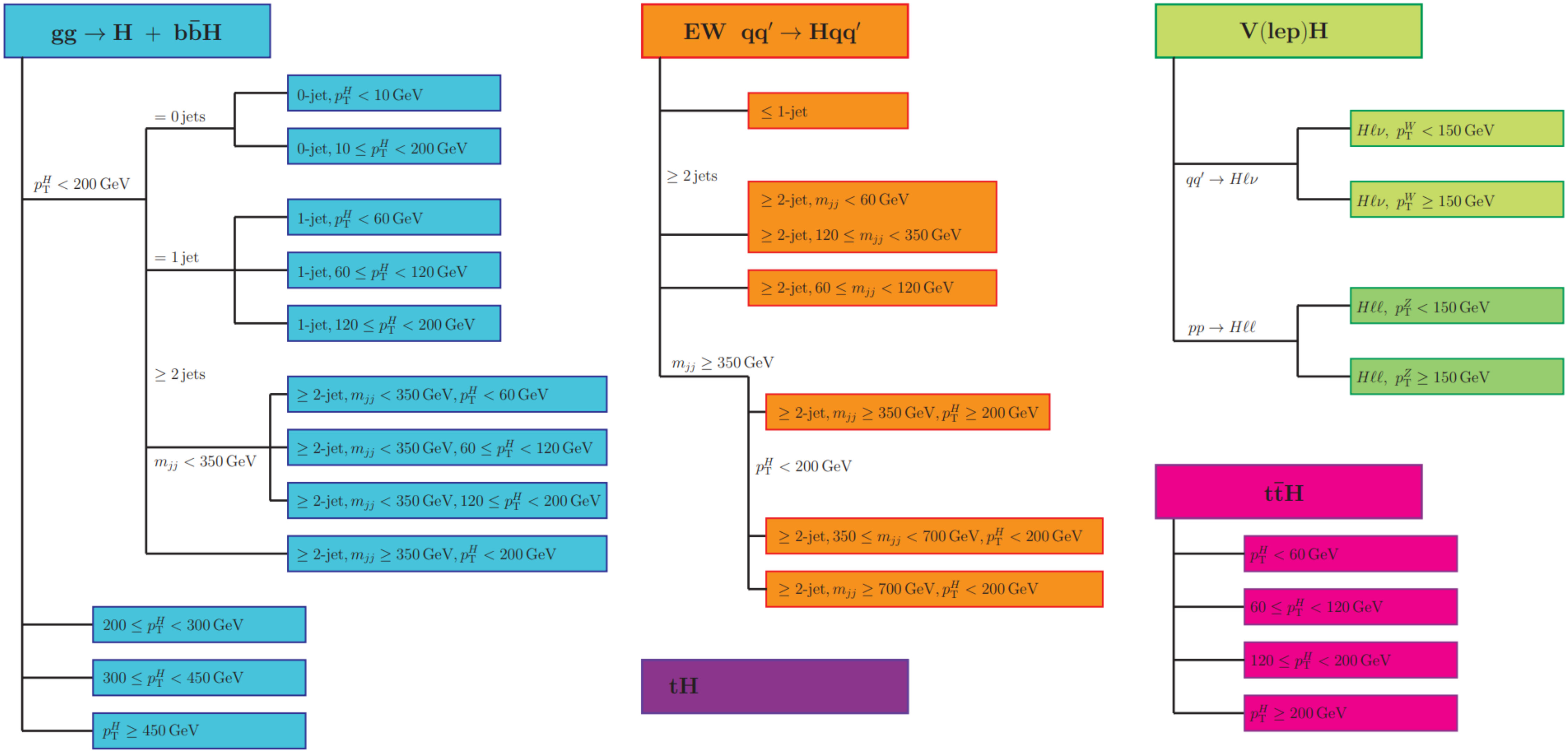

$gg \to H + b\bar{b}H$

- $p_T^H < 200$ GeV
  - $= 0$ jets
    - 0-jet, $p_T^H < 10$ GeV
    - 0-jet, $10 \leq p_T^H < 200$ GeV
  - $= 1$ jet
    - 1-jet, $p_T^H < 60$ GeV
    - 1-jet, $60 \leq p_T^H < 120$ GeV
    - 1-jet, $120 \leq p_T^H < 200$ GeV
  - ≥ 2 jets
    - $m_{jj} < 350$ GeV
      - $\geq$ 2-jet, $m_{jj} < 350$ GeV, $p_T^H < 60$ GeV
      - $\geq$ 2-jet, $m_{jj} < 350$ GeV, $60 \leq p_T^H < 120$ GeV
      - $\geq$ 2-jet, $m_{jj} < 350$ GeV, $120 \leq p_T^H < 200$ GeV
    - $\geq$ 2-jet, $m_{jj} \geq 350$ GeV, $p_T^H < 200$ GeV
- $200 \leq p_T^H < 300$ GeV
- $300 \leq p_T^H < 450$ GeV
- $p_T^H \geq 450$ GeV

EW $qq' \to Hqq'$

- $\leq$ 1-jet
- ≥ 2 jets
  - $\geq$ 2-jet, $m_{jj} < 60$ GeV
$\geq$ 2-jet, $120 \leq m_{jj} < 350$ GeV
  - $\geq$ 2-jet, $60 \leq m_{jj} < 120$ GeV
  - $m_{jj} \geq 350$ GeV
    - $\geq$ 2-jet, $m_{jj} \geq 350$ GeV, $p_T^H \geq 200$ GeV
    - $p_T^H < 200$ GeV
      - $\geq$ 2-jet, $350 \leq m_{jj} < 700$ GeV, $p_T^H < 200$ GeV
      - $\geq$ 2-jet, $m_{jj} \geq 700$ GeV, $p_T^H < 200$ GeV

tH

V(lep)H

- $qq' \to H\ell\nu$
  - $H\ell\nu$, $p_T^W < 150$ GeV
  - $H\ell\nu$, $p_T^W \geq 150$ GeV
- $pp \to H\ell\ell$
  - $H\ell\ell$, $p_T^Z < 150$ GeV
  - $H\ell\ell$, $p_T^Z \geq 150$ GeV

$t\bar{t}H$

- $p_T^H < 60$ GeV
- $60 \leq p_T^H < 120$ GeV
- $120 \leq p_T^H < 200$ GeV
- $p_T^H \geq 200$ GeV

Analysis

Photon reconstruction

- Reconstruct two photons: energy deposit in EM calorimeter.

Photon reconstruction

- Reconstruct two photons: energy deposit in EM calorimeter.

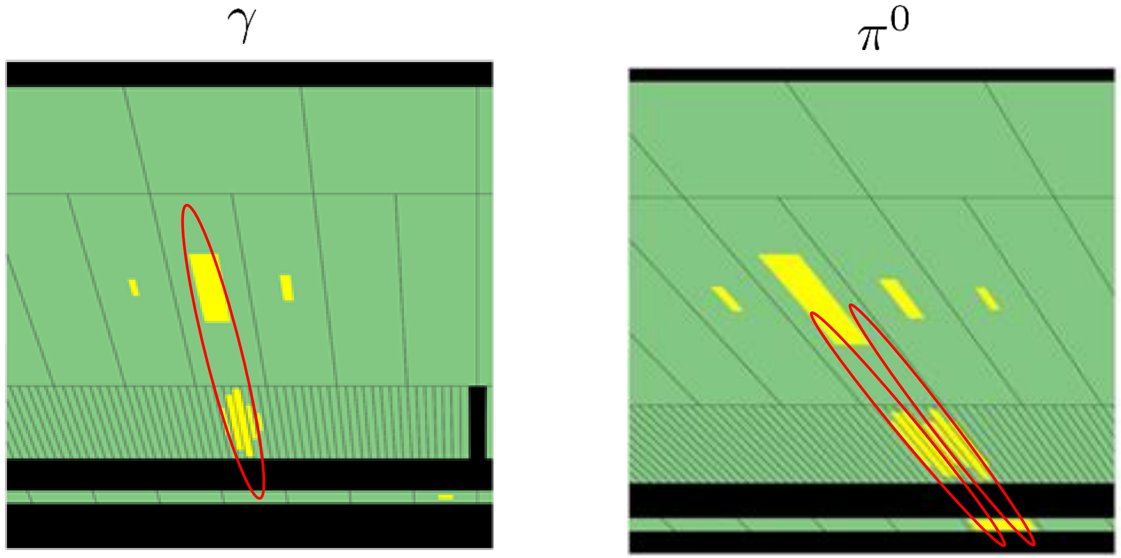

- **Jets** can mimic **photons**: exploit granularity to reject & shower-shape variables

Photon reconstruction

- Reconstruct two photons: energy deposit in EM calorimeter.

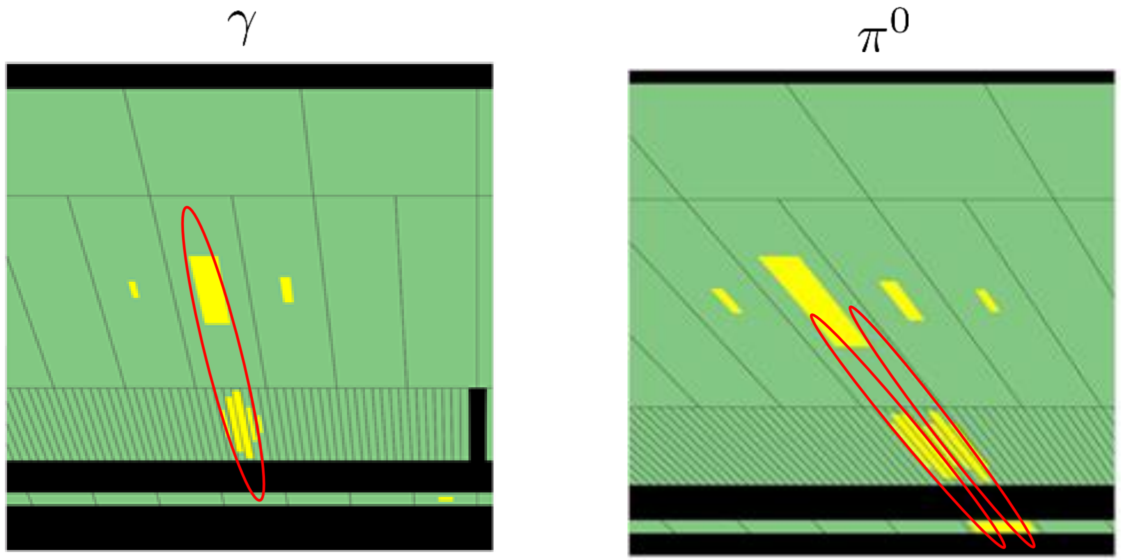

- **Jets** can mimic **photons**: exploit granularity to reject & shower-shape variables

Selection for photons:

$$|\eta| < 2.37,\ \text{excluding}\ |\eta| \in [1.37, 1.52]$$

$$\frac{E_T^{1(2)}}{m_{\gamma\gamma}} > 0.35\ (0.25)$$ + **tight** ID & isolation

Efficiency:
84% at pT = 25 GeV
94% at pT = 100 GeV

$m_{\gamma\gamma}$ spectrum

O**(6500) Higgs** bosons decaying **into two photons** in the full Run 2 dataset (139 fb-1) are available for analysis

Efficiency for an SM Higgs boson in $|y_H| < 2.5 \approx 39\%$

Need to precisely model signal & background

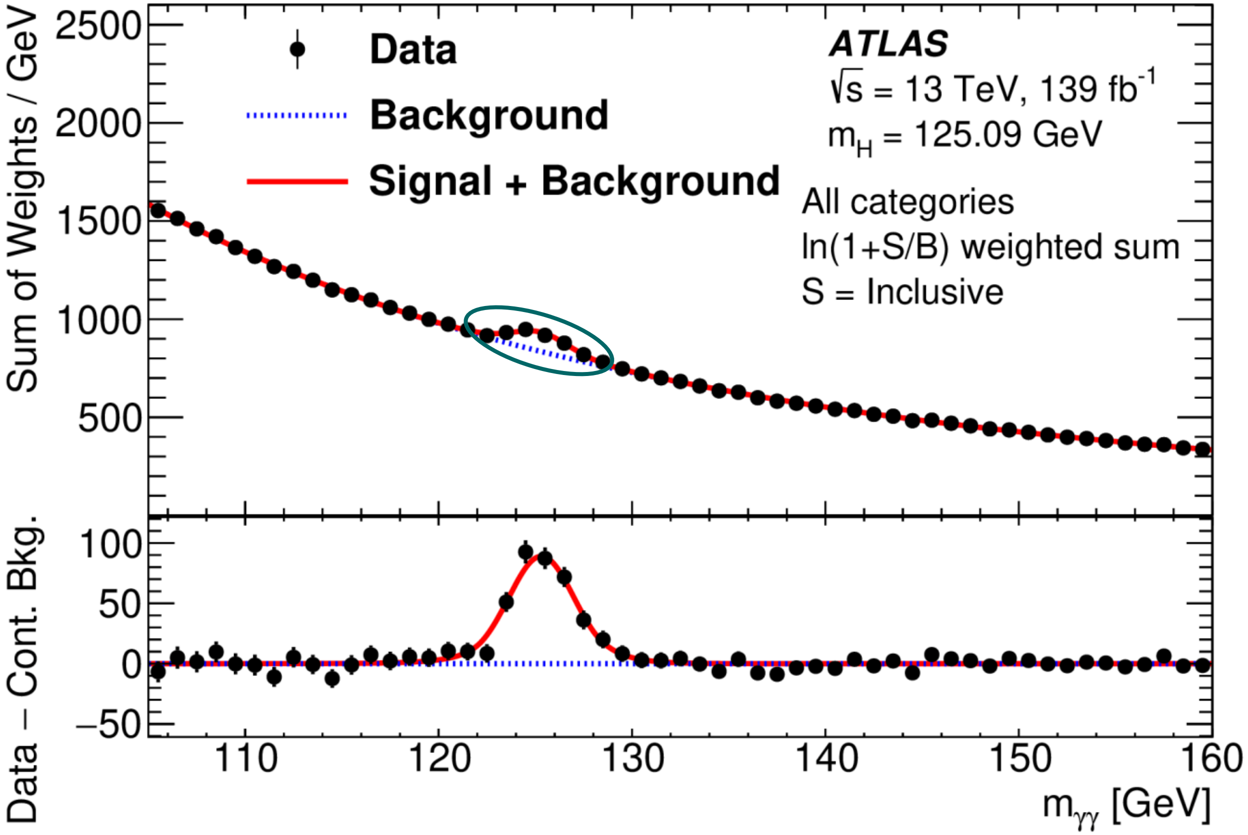

Statistical model

Extended term: fluctuation in the number of events

$$\mathcal{L}\left(\vec{\mu},\vec{\theta}|m_{\gamma\gamma}\right) = \boxed{\prod_c \mathrm{Pois}\left(n_c|\nu_c(\vec{\mu},\vec{\theta})\right)} \prod_i f_c(m^i_{\gamma\gamma}|\vec{\theta}) \times \prod_j G(\theta_j)$$

Statistical model

Extended term: fluctuation in the number of events

Diphoton mass Pdf

$$\mathcal{L}\left(\vec{\mu},\vec{\theta}|m_{\gamma\gamma}\right) = \boxed{\prod_{c}\mathrm{Pois}\left(n_c|\nu_c(\vec{\mu},\vec{\theta}\right)}\,\boxed{\prod_{i} f_c(m^{i}_{\gamma\gamma}|\vec{\theta})}\times\prod_{j} G(\theta_j)$$

Statistical model

Extended term: fluctuation in the number of events

Diphoton mass Pdf

$$\mathcal{L}\left(\vec{\mu},\vec{\theta}|m_{\gamma\gamma}\right) = \boxed{\prod_{c} \mathrm{Pois}\left(n_c|\nu_c(\vec{\mu},\vec{\theta}\right)} \boxed{\prod_{i} f_c(m^{i}_{\gamma\gamma}|\vec{\theta})} \times \prod_{j} G(\theta_j)$$

Diphoton mass Pdf for given category c:

$$f_c(m_{\gamma\gamma}{}^{i}|\vec{\theta}) = \frac{1}{\nu_c}\left\{\left[s_c\left(\vec{\mu},\vec{\theta}\right)+N^{c}_{sp}\vec{\theta}^{c}_{sp}\right]\mathrm{Pdf}^{c}_{sig}\left(m_{\gamma\gamma}|\vec{\theta}_{sp}\right)+b_c\mathrm{Pdf}^{c}_{bkg}(m_{\gamma\gamma}|\vec{\theta}_{bkg})\right\}$$

Statistical model

Extended term: fluctuation in the number of events

Diphoton mass Pdf

$$\mathcal{L}\left(\vec{\mu},\vec{\theta}|m_{\gamma\gamma}\right) = \boxed{\prod_{c}\mathrm{Pois}\left(n_c|\nu_c(\vec{\mu},\vec{\theta}\right)} \boxed{\prod_{i} f_c(m^{i}_{\gamma\gamma}|\vec{\theta})} \times \prod_{j} G(\theta_j)$$

Diphoton mass Pdf for given category c:

$$f_c(m_{\gamma\gamma}{}^{i}|\vec{\theta}) = \frac{1}{\nu_c}\left\{\left[\boxed{s_c}\left(\vec{\mu},\vec{\theta}\right)+N^{c}_{sp}\vec{\theta}^{c}_{sp}\right]\mathrm{Pdf}^{c}_{sig}\left(m_{\gamma\gamma}|\vec{\theta}_{sp}\right)+b_c\mathrm{Pdf}^{c}_{bkg}(m_{\gamma\gamma}|\vec{\theta}_{bkg})\right\}$$

Fitted signal

$$\nu_c = s_c + N^{c}_{sp} + b_c$$

$$s_c = \sum_{c}\sigma_t\mathcal{A}_{ct}\varepsilon_{ct}\mathcal{L}$$

Luminosity

Efficiency

Acceptance

Cross-section of truth-bin

Statistical model

Extended term: fluctuation in the number of events

Diphoton mass Pdf

$$\mathcal{L}\left(\vec{\mu},\vec{\theta}|m_{\gamma\gamma}\right) = \boxed{\prod_c \mathrm{Pois}\left(n_c|\nu_c(\vec{\mu},\vec{\theta})\right)}\boxed{\prod_i f_c(m^i_{\gamma\gamma}|\vec{\theta})} \times \prod_j G(\theta_j)$$

Diphoton mass Pdf for given category c:

$$f_c({m_{\gamma\gamma}}^i|\vec{\theta}) = \frac{1}{\nu_c}\left\{\left[\boxed{s_c}\left(\vec{\mu},\vec{\theta}\right)+\boxed{N^c_{sp}}\vec{\theta}^c_{sp}\right]\mathrm{Pdf}^c_{sig}\left(m_{\gamma\gamma}|\vec{\theta}_{sp}\right)+b_c\mathrm{Pdf}^c_{bkg}(m_{\gamma\gamma}|\vec{\theta}_{bkg})\right\}$$

spurious signal

Fitted signal

$$\nu_c = s_c + N^c_{sp} + b_c$$

$$s_c = \sum_c \sigma_t \mathcal{A}_{ct} \varepsilon_{ct} \mathcal{L}$$

Luminosity

Efficiency

Acceptance

Cross-section of truth-bin

Statistical model

Extended term: fluctuation in the number of events

Diphoton mass Pdf

$$\mathcal{L}\left(\vec{\mu},\vec{\theta}|m_{\gamma\gamma}\right) = \boxed{\prod_c \mathrm{Pois}\left(n_c|\nu_c(\vec{\mu},\vec{\theta})\right)}\boxed{\prod_i f_c(m^i_{\gamma\gamma}|\vec{\theta})} \times \prod_j G(\theta_j)$$

Diphoton mass Pdf for given category c:

$$f_c({m_{\gamma\gamma}}^i|\vec{\theta}) = \frac{1}{\nu_c}\left\{\left[\boxed{s_c}\left(\vec{\mu},\vec{\theta}\right)+\boxed{N^c_{sp}}\vec{\theta}^c_{sp}\right]\mathrm{Pdf}^c_{sig}\left(m_{\gamma\gamma}|\vec{\theta}_{sp}\right)+\boxed{b_c}\mathrm{Pdf}^c_{bkg}(m_{\gamma\gamma}|\vec{\theta}_{bkg})\right\}$$

Fitted bkg

spurious signal

Fitted signal

$$\nu_c = s_c + N^c_{sp} + b_c$$

$$s_c = \sum_c \sigma_t \mathcal{A}_{ct} \varepsilon_{ct} \mathcal{L}$$

Luminosity

Efficiency

Acceptance

Cross-section of truth-bin

Statistical model

Extended term: fluctuation in the number of events

Diphoton mass Pdf

Constrains on systematics

$$\mathcal{L}\left(\vec{\mu},\vec{\theta}|m_{\gamma\gamma}\right) = \boxed{\prod_c \mathrm{Pois}\left(n_c|\nu_c(\vec{\mu},\vec{\theta})\right)}\boxed{\prod_i f_c(m^i_{\gamma\gamma}|\vec{\theta})} \times \boxed{\prod_j G(\boxed{\theta_j})}$$

Nuisance parameters

Diphoton mass Pdf for given category c:

$$f_c({m_{\gamma\gamma}}^i|\vec{\theta}) = \frac{1}{\nu_c}\left\{\left[\boxed{s_c}\left(\vec{\mu},\vec{\theta}\right)+\boxed{N^c_{sp}}\vec{\theta}^c_{sp}\right]\mathrm{Pdf}^c_{sig}\left(m_{\gamma\gamma}|\vec{\theta}_{sp}\right)+\boxed{b_c}\mathrm{Pdf}^c_{bkg}(m_{\gamma\gamma}|\vec{\theta}_{bkg})\right\}$$

Fitted bkg

spurious signal

Fitted signal

$$\nu_c = s_c + N^c_{sp} + b_c$$

$$s_c = \sum_c \sigma_t \mathcal{A}_{ct} \varepsilon_{ct} \mathcal{L}$$

Luminosity

Efficiency

Acceptance

Cross-section of truth-bin

Statistical model

Extended term: fluctuation in the number of events

Diphoton mass Pdf

Constrains on systematics

$$\mathcal{L}\left(\vec{\mu},\vec{\theta}|m_{\gamma\gamma}\right) = \boxed{\prod_c \mathrm{Pois}\left(n_c|\nu_c(\vec{\mu},\vec{\theta})\right)}\boxed{\prod_i f_c(m^i_{\gamma\gamma}|\vec{\theta})} \times \boxed{\prod_j G(\boxed{\theta_j})}$$

Nuisance parameters

Diphoton mass Pdf for given category c:

$$f_c({m_{\gamma\gamma}}^i|\vec{\theta}) = \frac{1}{\nu_c}\left\{\left[\boxed{s_c}\left(\vec{\mu},\vec{\theta}\right)+\boxed{N^c_{sp}}\vec{\theta}^c_{sp}\right]\mathrm{Pdf}^c_{sig}\left(m_{\gamma\gamma}|\vec{\theta}_{sp}\right)+\boxed{b_c}\mathrm{Pdf}^c_{bkg}(m_{\gamma\gamma}|\vec{\theta}_{bkg})\right\}$$

Fitted bkg

spurious signal

Fitted signal

$$\nu_c = s_c + N^c_{sp} + b_c$$

$$s_c = \sum_c \sigma_t \mathcal{A}_{ct} \varepsilon_{ct} \mathcal{L}$$

Luminosity

Efficiency

Acceptance

Cross-section of truth-bin

Simultaneous fit of **101 categories**, targeting 28 truth bins

~300 parameters

~400 systematics

STXS measurement

101 categories targeting **28 truth bins**

Categorisation:

- **Multiclass BDT** to assign events to the targeted truth bins
- **Binary BDT** to separate signal from bkg

Pairing:

Reconstructed category <=> **truth** bin

STXS Purity plot

Categories are **merged** only **for visualisation**

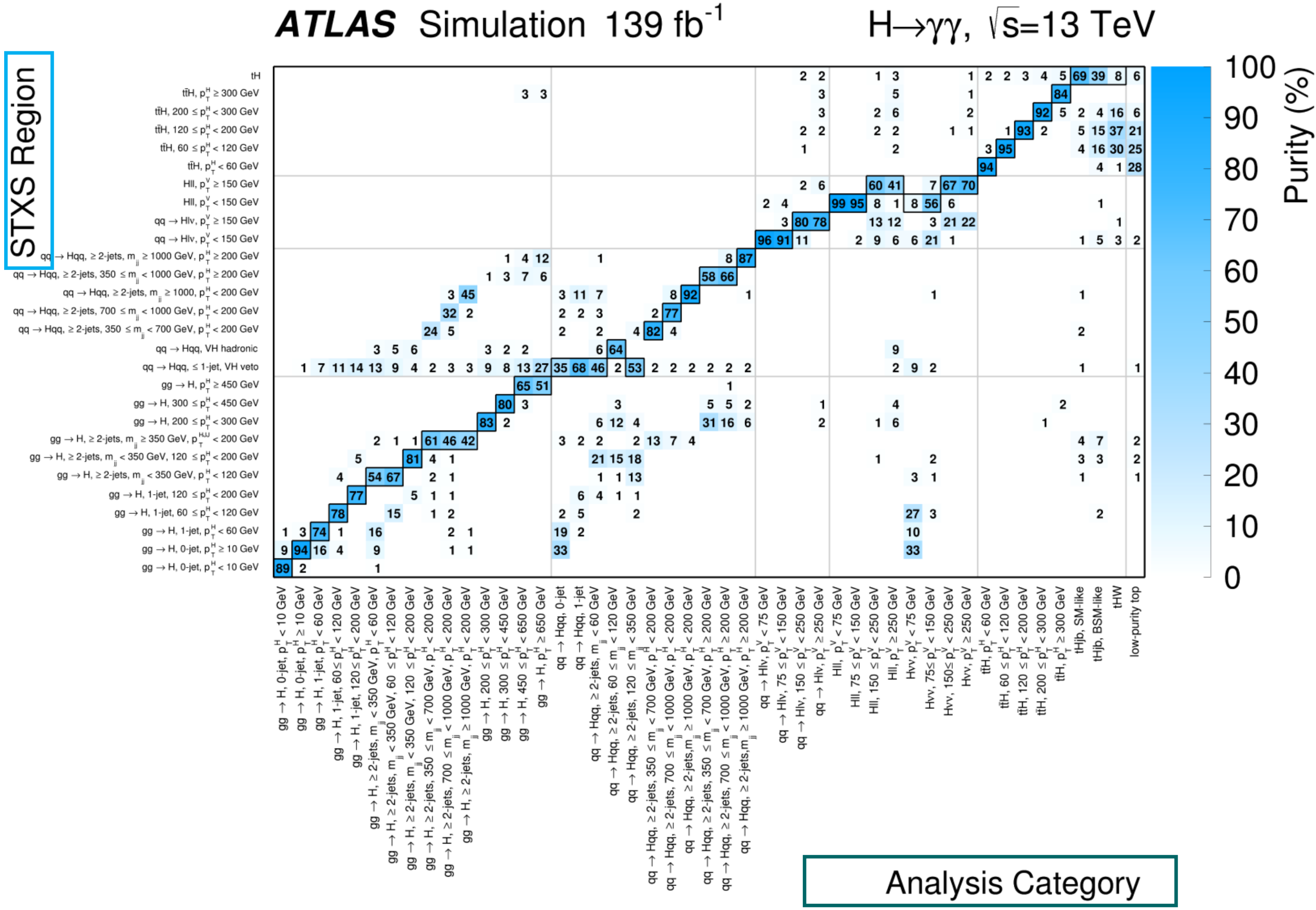

Signal shape modelling

From MC simulation

Double-Sided Crystal Ball function:
Gaussian core + asymmetric polynomial tails

Unbinned Likelihood fit, fixed range:
113-138 GeV

Independently for each of the 101 **categories**

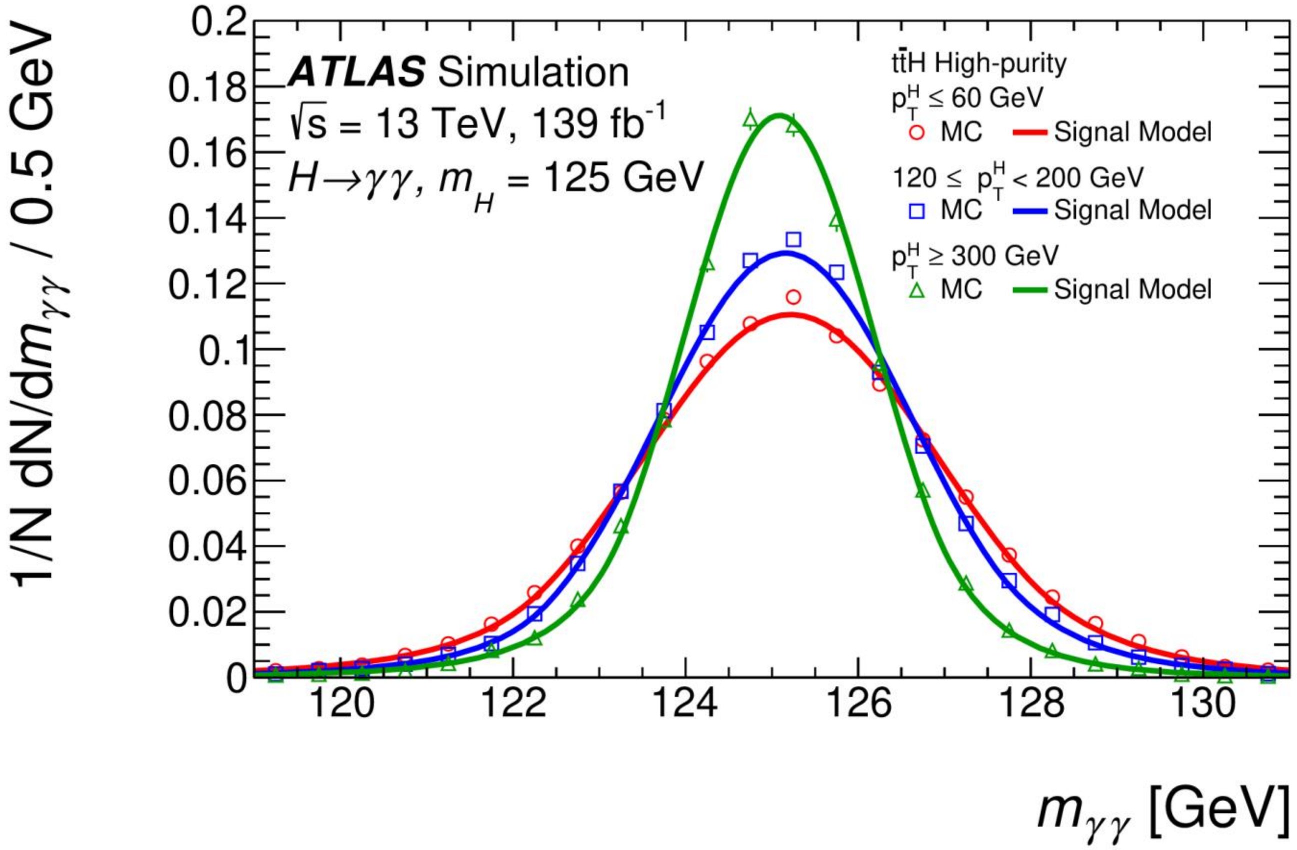

Background Modelling

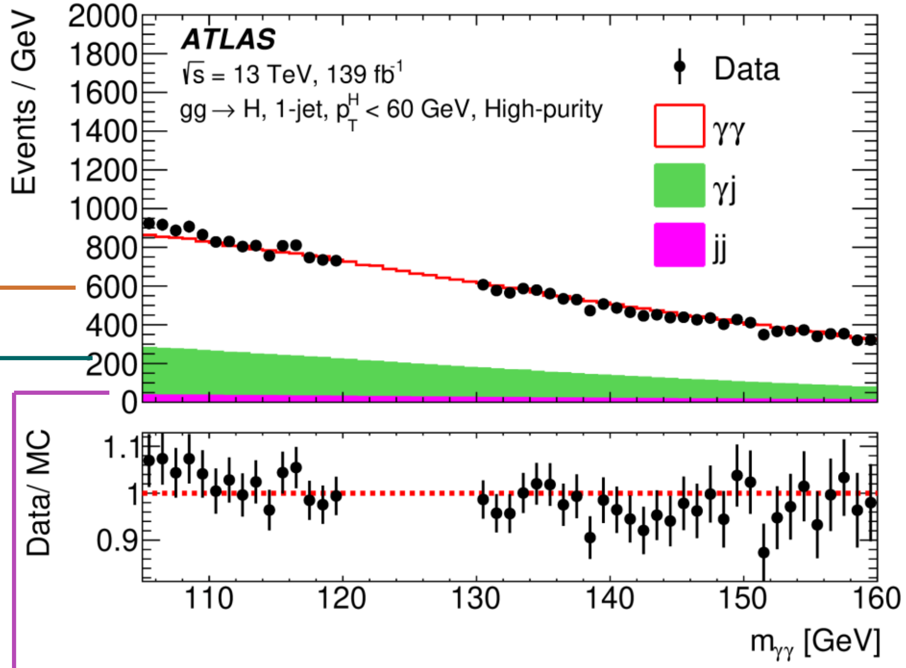

Background components:

- yy 80%

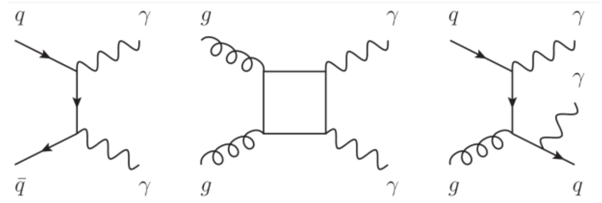

- yj 18%

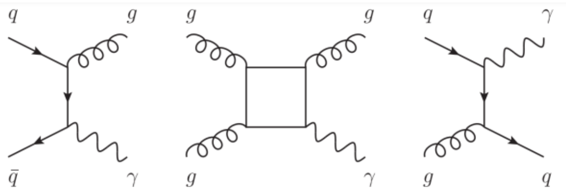

- jj 2%

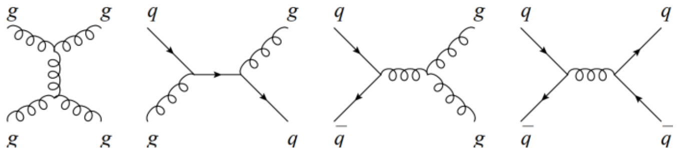

Background: yy + yj + jj.

Directly estimated from data with ABCD method

Background Modelling

Background components:

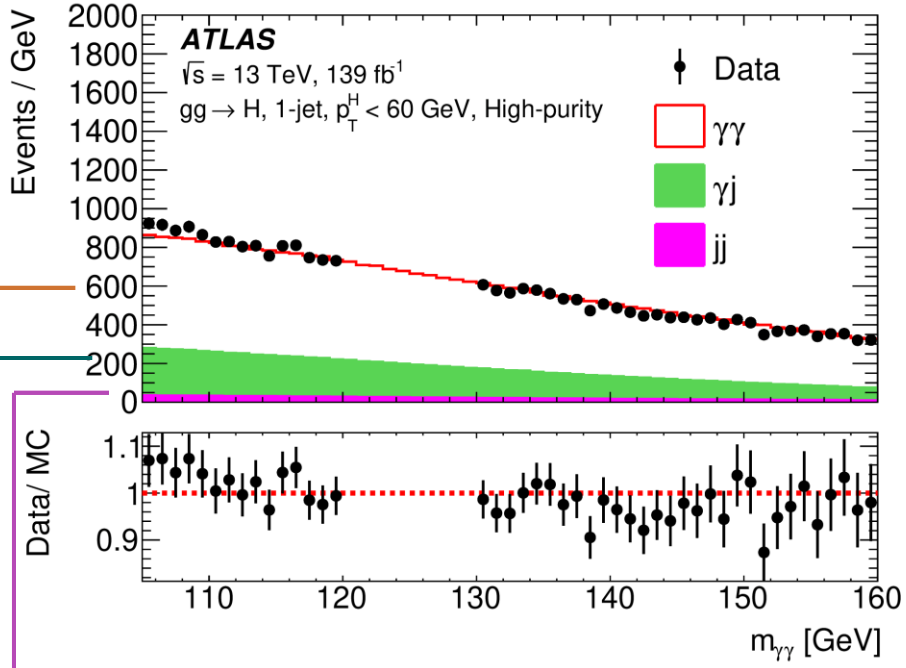

- yy 80%

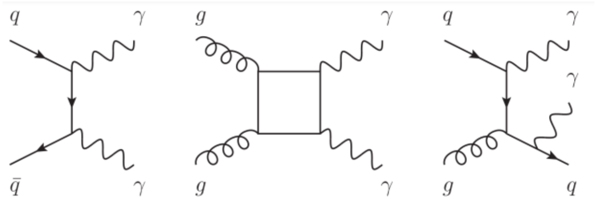

- yj 18%

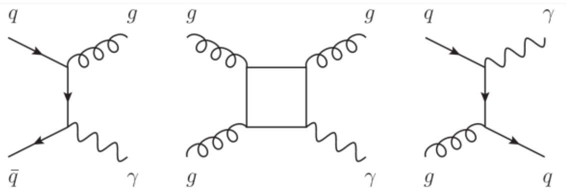

- jj 2%

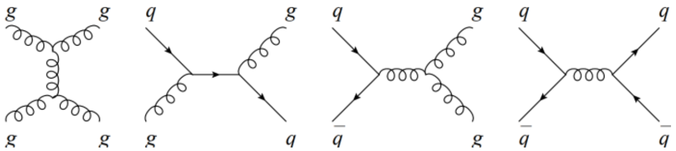

Background: yy + yj + jj.

- Jets Bkg modelling is complex and computationally expensive:

Directly estimated from data with ABCD method

Background Modelling

Background components:

- yy 80%

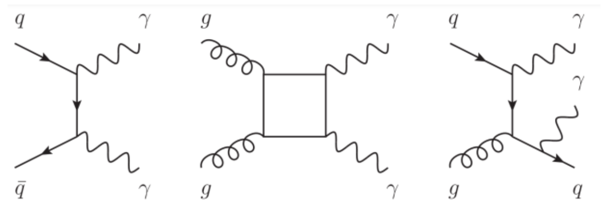

- yj 18%

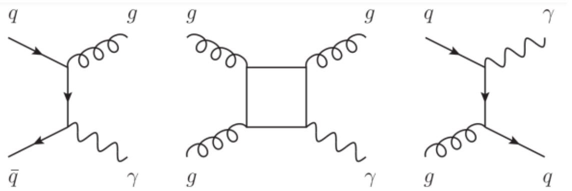

- jj 2%

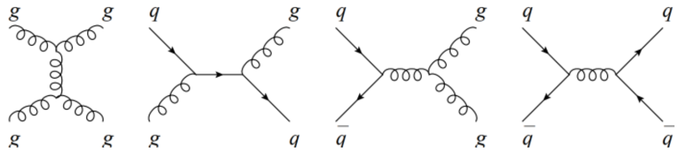

Background: yy + yj + jj.

- Jets Bkg modelling is complex and computationally expensive:
- Use yy template re-weighted to the shape of yj and jj in the data

Directly estimated from data with ABCD method

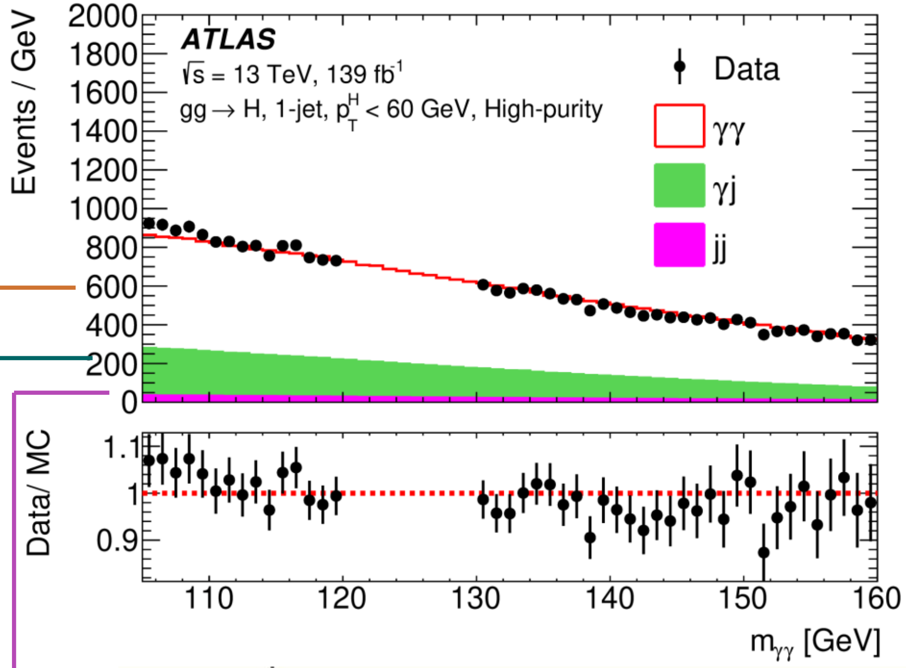

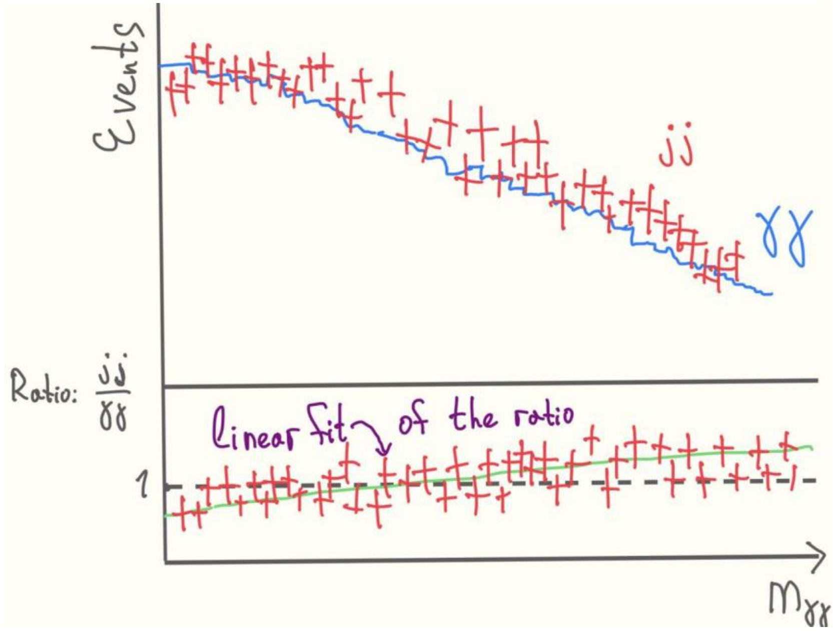

Background Modelling

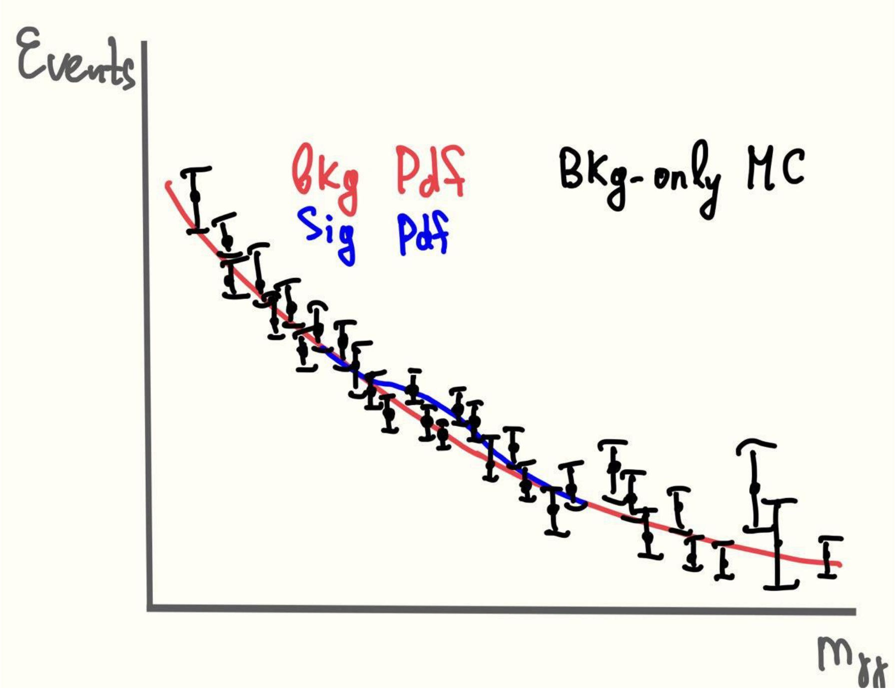

Functional form (exp, Bernstein, polynomial) is chosen by Spurious signal test or Wald test (low-stat categories):

Background Modelling

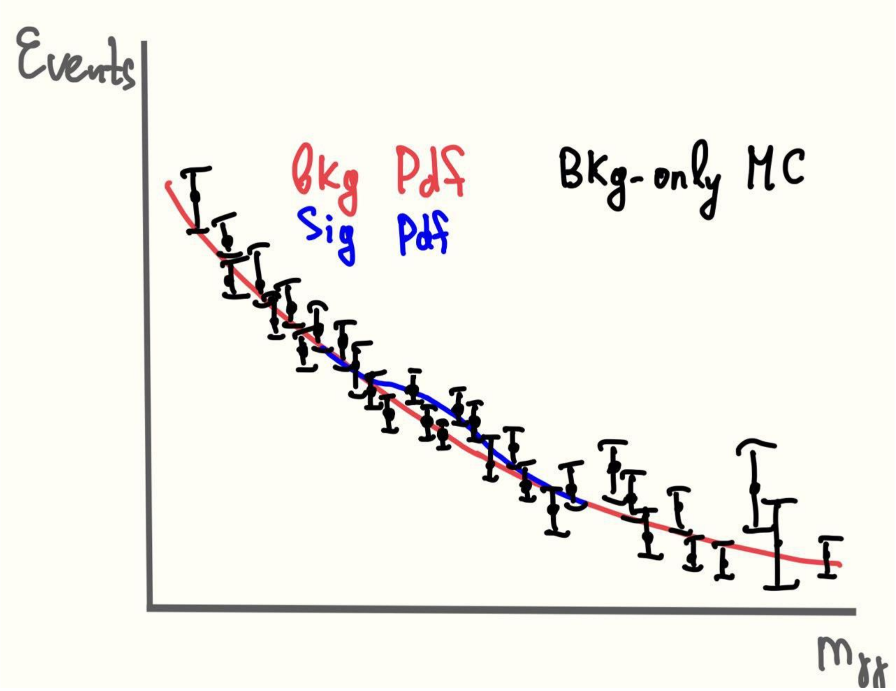

Functional form (exp, Bernstein, polynomial) is chosen by Spurious signal test or Wald test (low-stat categories):

Try a series of fits:

- bkg-only MC with (bkg + sig) pdf
- Signal at various positions (123-127 GeV) with 0.5 GeV step

Background Modelling

Functional form (exp, Bernstein, polynomial) is chosen by Spurious signal test or Wald test (low-stat categories):
Try a series of fits:

- bkg-only MC with (bkg + sig) pdf
- Signal at various positions (123-127 GeV) with 0.5 GeV step

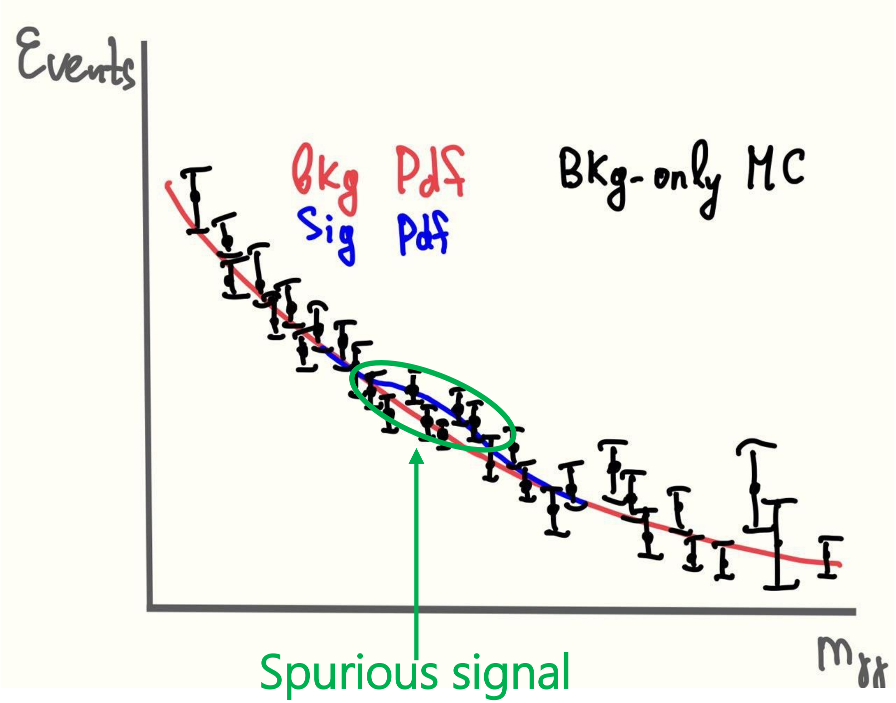

Spurious signal

Background Modelling

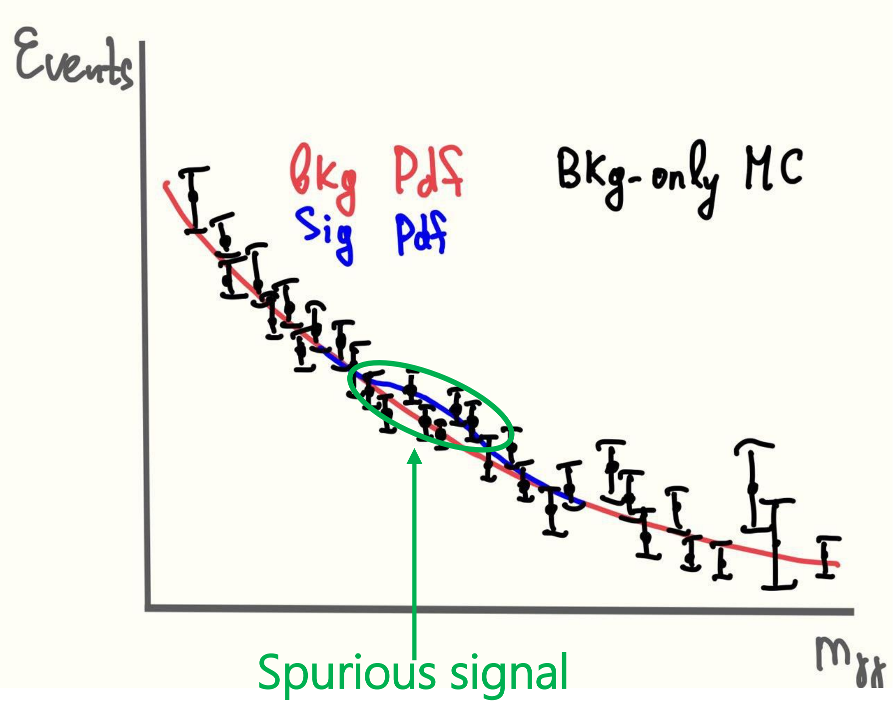

Spurious signal

Functional form (exp, Bernstein, polynomial) is chosen by Spurious signal test or Wald test (low-stat categories):
Try a series of fits:

- bkg-only MC with (bkg + sig) pdf
- Signal at various positions (123-127 GeV) with 0.5 GeV step

- Take the one with the lowest # params passing criteria:
  N_sp < 10% expected signal
  N_sp < 20% expected error on bkg (for Asimov dataset)

Background Modelling

Functional form (exp, Bernstein, polynomial) is chosen by Spurious signal test or Wald test (low-stat categories):
Try a series of fits:

- bkg-only MC with (bkg + sig) pdf
- Signal at various positions (123-127 GeV) with 0.5 GeV step

- Take the one with the lowest # params passing criteria:
  N_sp < 10% expected signal
  N_sp < 20% expected error on bkg (for Asimov dataset)

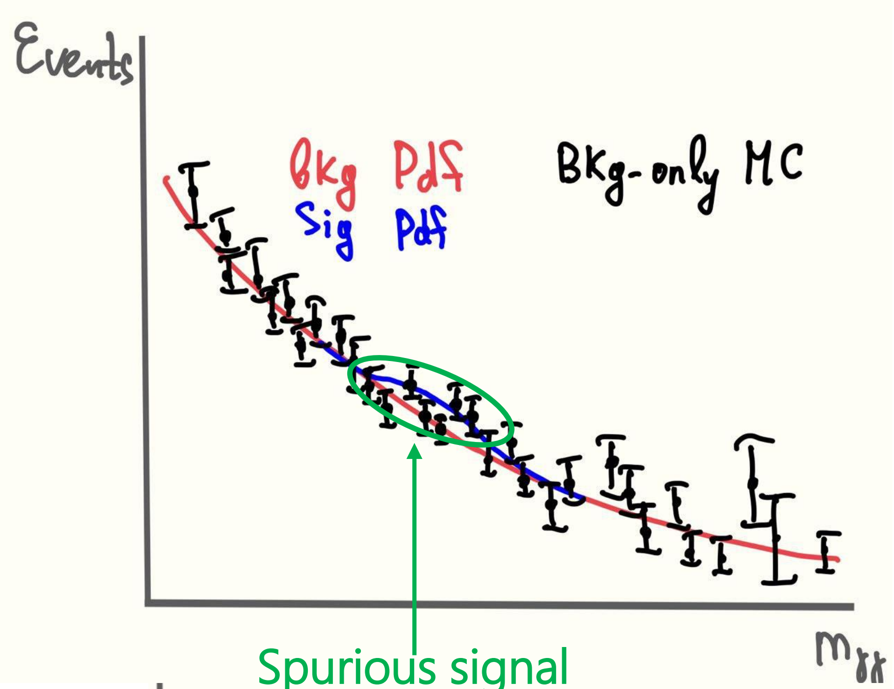

Spurious signal

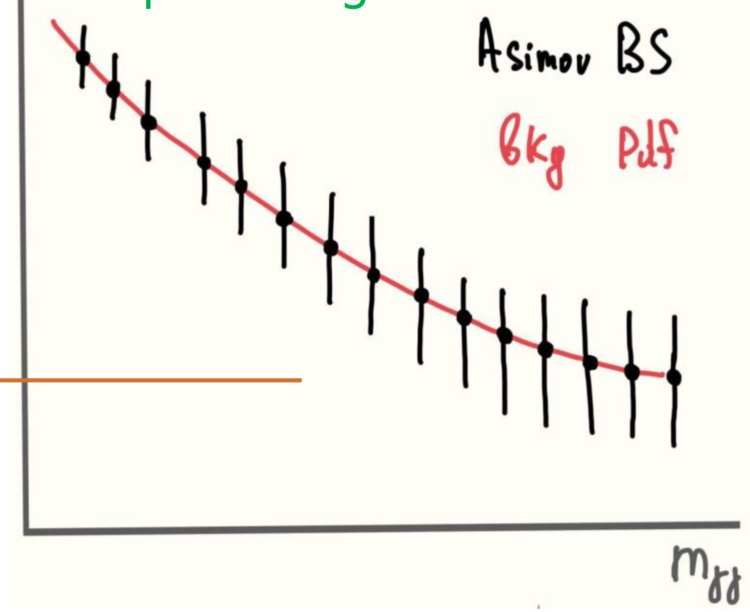

Results: signal strengths

Inclusive

$$\sigma^{\gamma\gamma}/\sigma^{\gamma\gamma}_{SM} = 1.045\,^{+0.084}_{-0.080} = 1.04\,^{+0.060}_{-0.059}\,(\text{stat.})\,^{+0.059}_{-0.054}\,(\text{syst.})$$

No significant deviations wrt SM

Results: signal strengths

Inclusive

$$\sigma^{\gamma\gamma}/\sigma^{\gamma\gamma}_{SM} = 1.045\,^{+0.084}_{-0.080} = 1.04\,^{+0.060}_{-0.059}\,(\text{stat.})\,^{+0.059}_{-0.054}\,(\text{syst.})$$

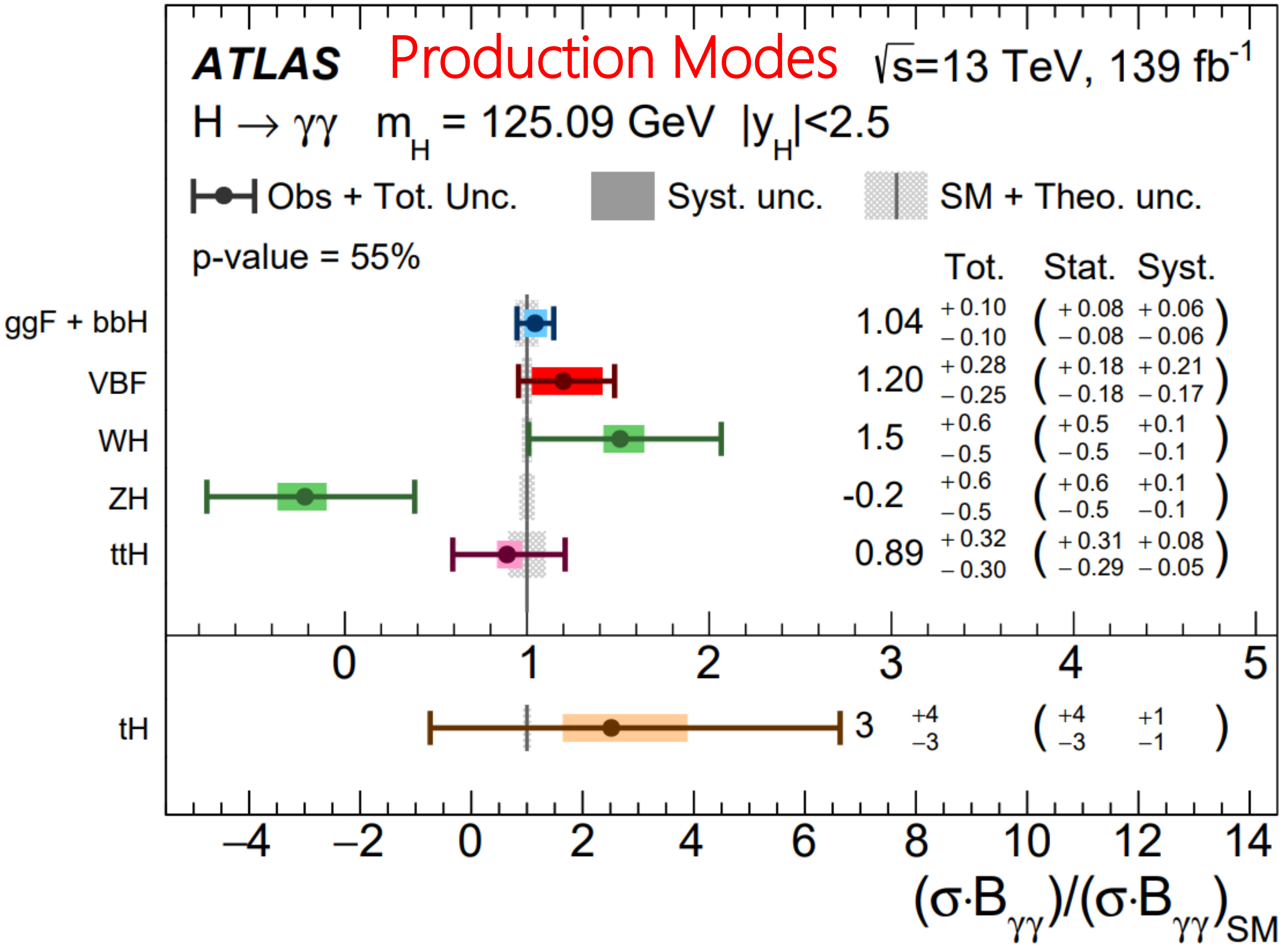

No significant deviations wrt SM

Results: signal strengths

Inclusive

$$\sigma^{\gamma\gamma}/\sigma^{\gamma\gamma}_{SM} = 1.045\ {}^{+0.084}_{-0.080} = 1.04\ {}^{+0.060}_{-0.059}\ (\text{stat.})\ {}^{+0.059}_{-0.054}\ (\text{syst.})$$

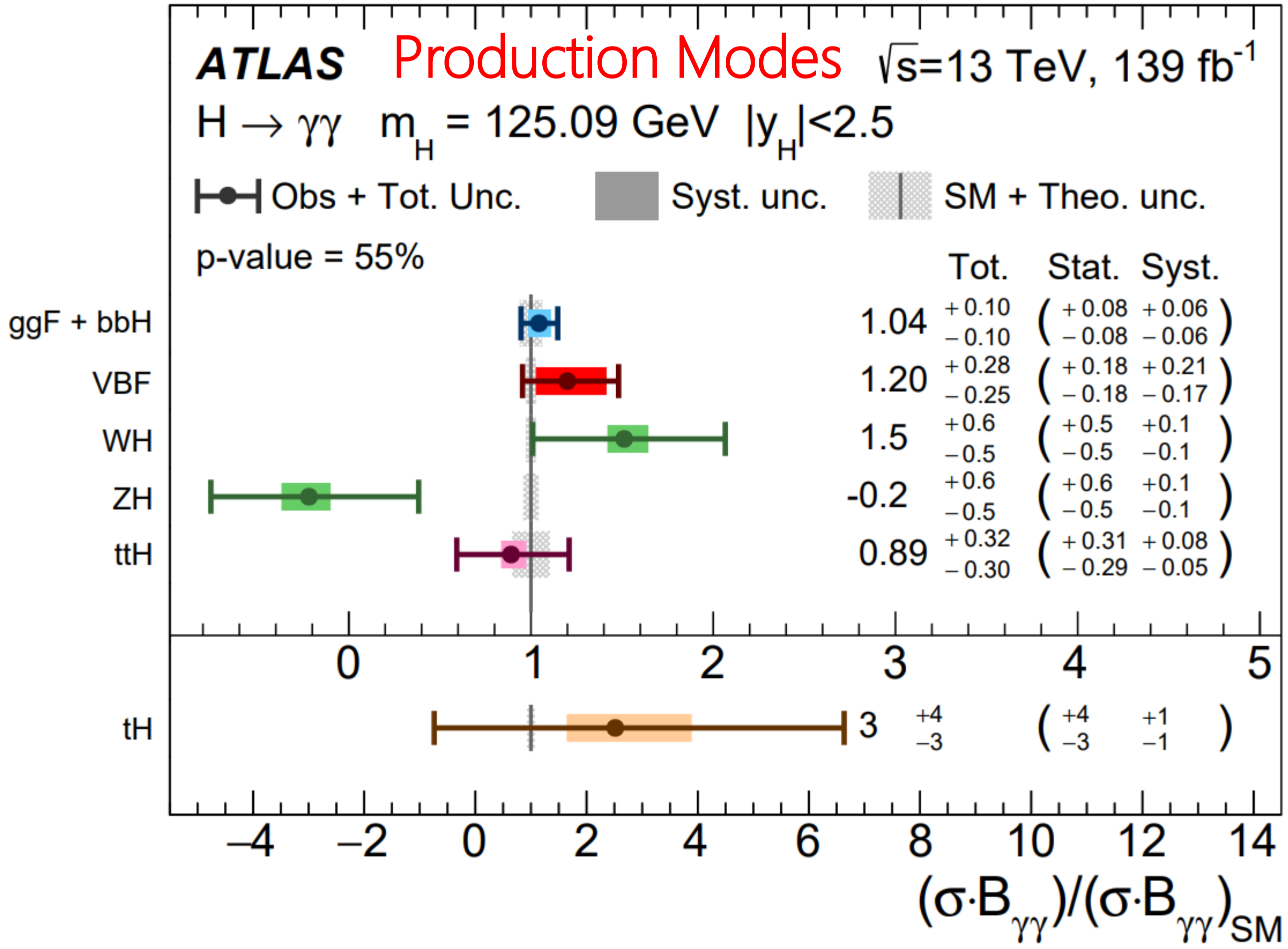
Production Modes

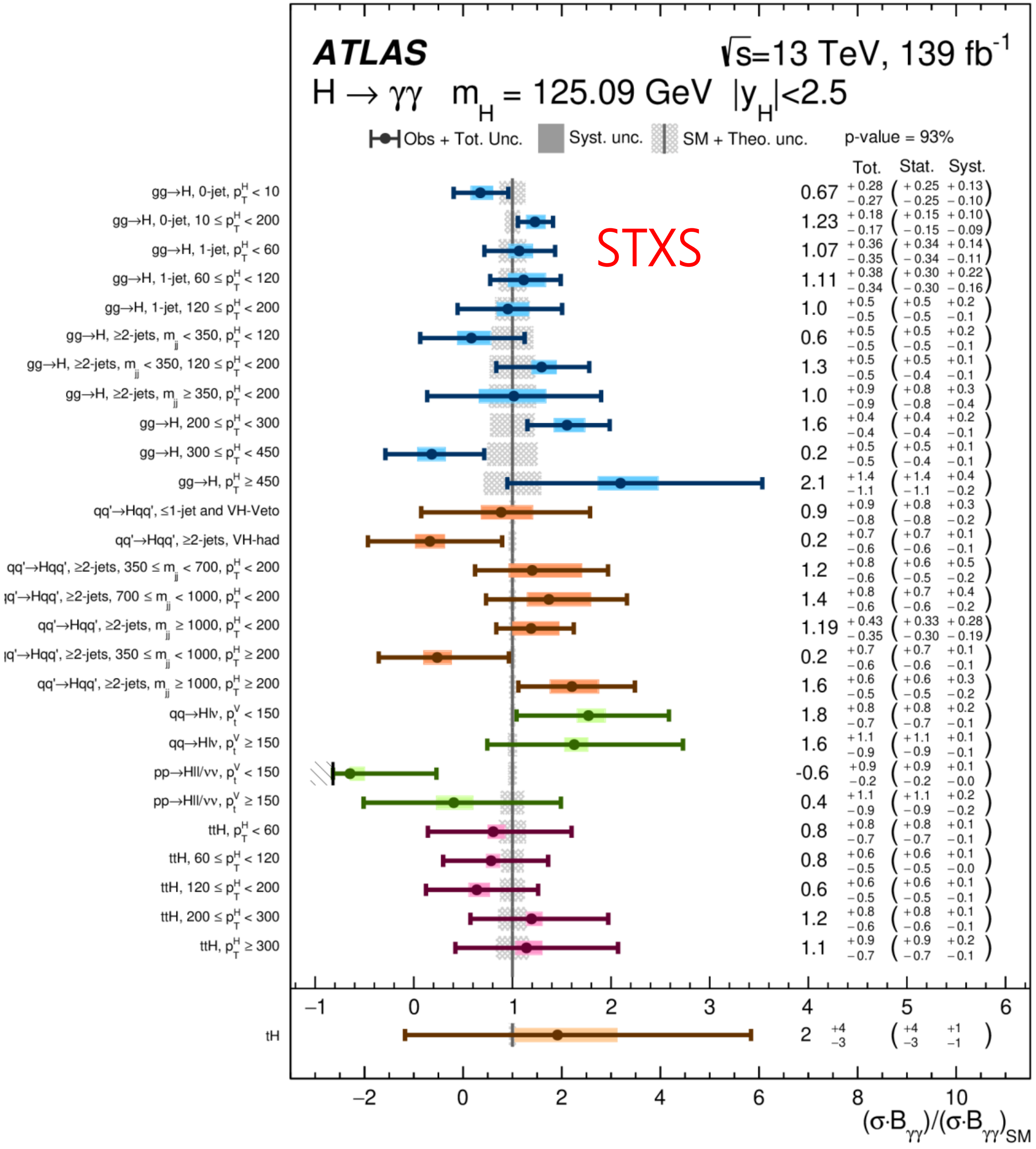
STXS

No significant deviation:

Results: Kappa-framework

Likelihood scans of the effective couplings (probing amplitudes):

Higgs-gluons vs Higgs-photons

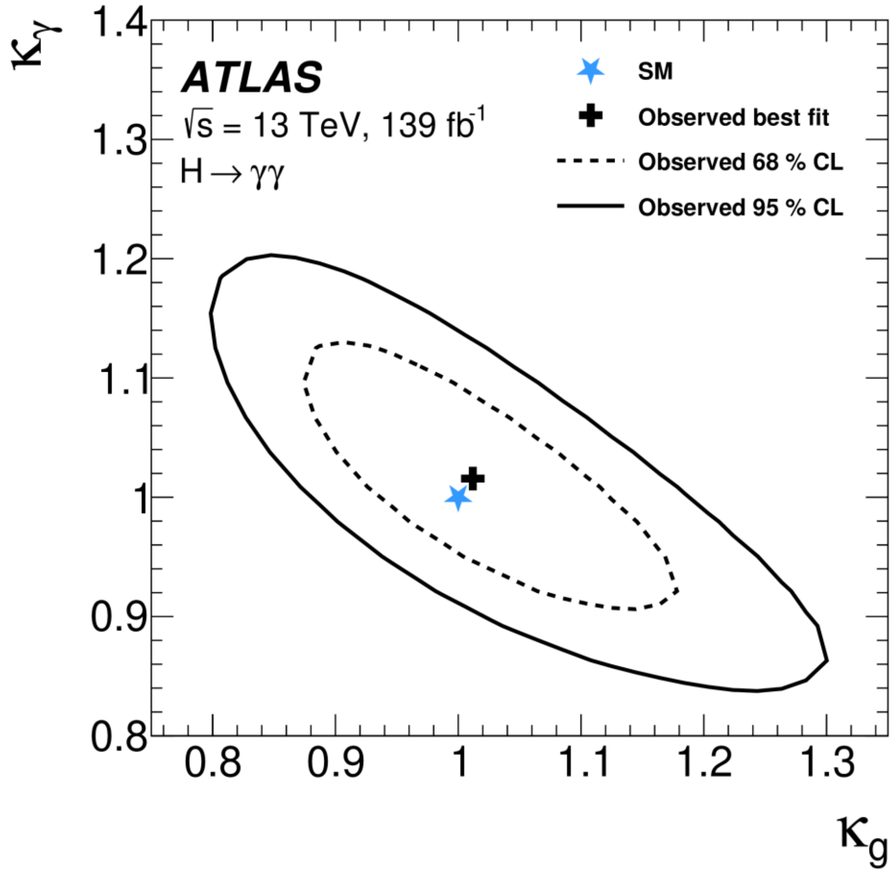

Higgs-fermions vs Higgs-vector bosons

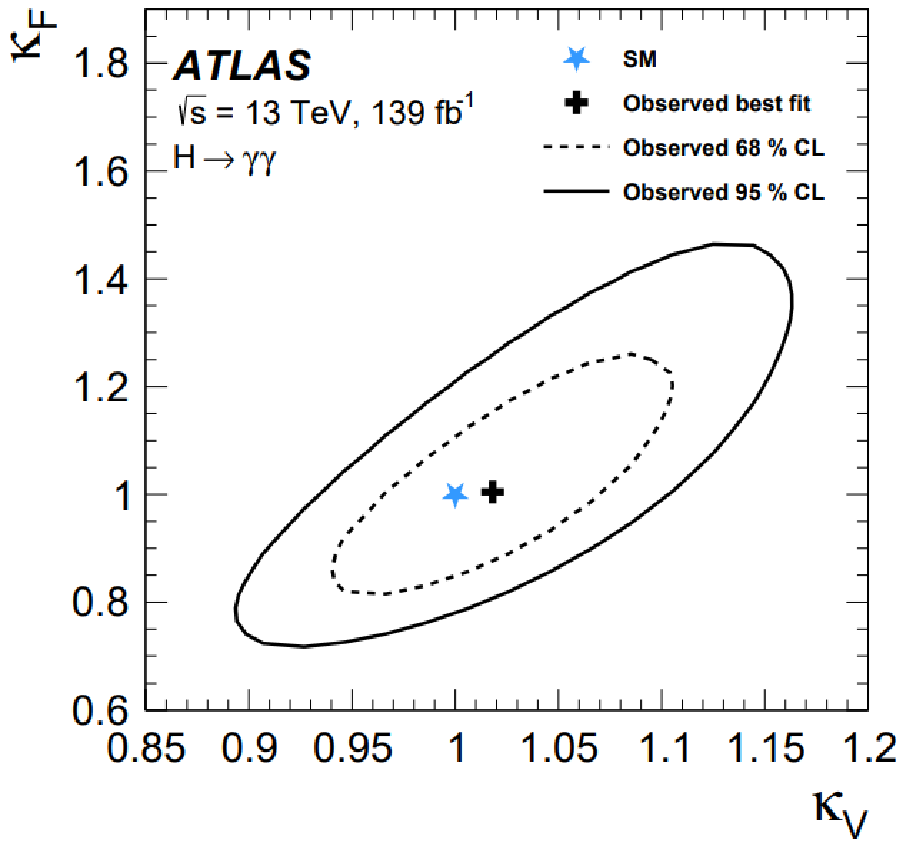

EFT interpretation

EFT interpretation: SMEFT (Standard Model Effective Field Theory)

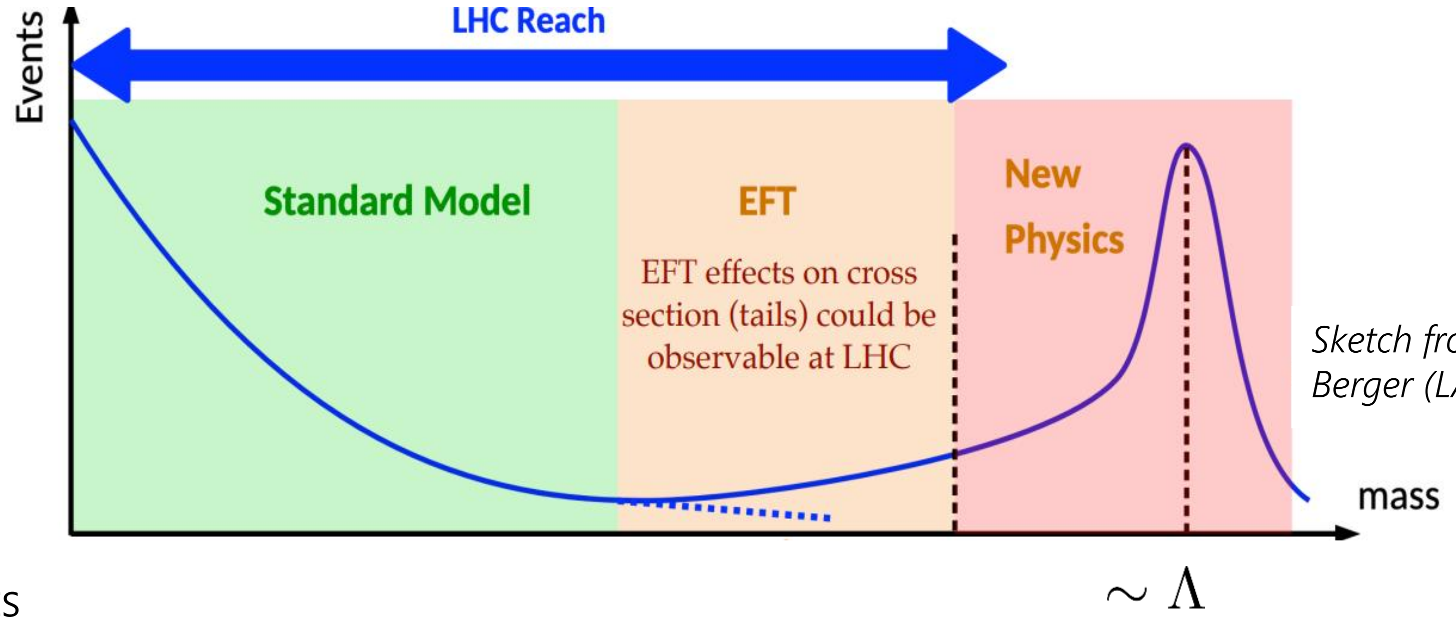

Sketch from Nicolas Berger (LAPP)

Wilson coefficients

$$\mathcal{L}_{SMEFT} = \boxed{\mathcal{L}_{SM}} + \sum \frac{\boxed{\mathcal{C}_k}}{\Lambda^2} \boxed{\mathcal{O}_k} + O(\boxed{\Lambda}^{-4})$$

Energy-scale of the new physics

Basis-operators formed from combinations of the SM operators

SM Lagrangian

EFT: Method

EFT impact on the cross-section of the truth bin t, decaying into final state f

$$\sigma^{t,f} = \sigma_{SM}^{t,f} + \sigma_{int}^{t,f} + \sigma_{BSM}^{t,f}$$

EFT: Method

EFT impact on the cross-section of the truth bin t, decaying into final state f

$$\sigma^{t,f} = \boxed{\sigma^{t,f}_{SM}} + \sigma^{t,f}_{int} + \sigma^{t,f}_{BSM}$$

Pure SM cross-section

EFT: Method

EFT impact on the cross-section of the truth bin t, decaying into final state f

$$\sigma^{t,f} = \boxed{\sigma^{t,f}_{SM}} + \boxed{\sigma^{t,f}_{int}} + \sigma^{t,f}_{BSM}$$

Interference SM-BSM

Pure SM cross-section

EFT: Method

EFT impact on the cross-section of the truth bin t, decaying into final state f

$$\sigma^{t,f} = \boxed{\sigma^{t,f}_{SM}} + \boxed{\sigma^{t,f}_{int}} + \boxed{\sigma^{t,f}_{BSM}}$$

Pure BSM contribution

Interference SM-BSM

Pure SM cross-section

EFT: Method

EFT impact on the cross-section of the truth bin t, decaying into final state f

$$\sigma^{t,f} = \boxed{\sigma^{t,f}_{SM}} + \boxed{\sigma^{t,f}_{int}} + \cancel{\sigma^{t,f}_{BSM}}$$

Pure BSM contribution

Interference SM-BSM

Pure SM cross-section

$$\sigma^{t,f} = \sigma^{t} \frac{\Gamma^{H\rightarrow f}}{\Gamma^{H}}$$

EFT: Method

EFT impact on the cross-section of the truth bin t, decaying into final state f

$$\sigma^{t,f} = \boxed{\sigma^{t,f}_{SM}} + \boxed{\sigma^{t,f}_{int}} + \cancel{\boxed{\sigma^{t,f}_{BSM}}}$$

Pure BSM contribution

Interference SM-BSM

Pure SM cross-section

Comparing:
Linear vs Linear + Quadratic
allows checking the possibility of neglecting dim 8 terms

$$\sigma^{t,f} = \sigma^{t} \frac{\Gamma^{H \to f}}{\Gamma^{H}}$$

EFT: Method

EFT impact on the cross-section of the truth bin t, decaying into final state f

$$\sigma^{t,f} = \boxed{\sigma^{t,f}_{SM}} + \boxed{\sigma^{t,f}_{int}} + \cancel{\boxed{\sigma^{t,f}_{BSM}}}$$

Pure BSM contribution

Interference SM-BSM

Pure SM cross-section

Comparing:
Linear vs Linear + Quadratic
allows checking the possibility of neglecting dim 8 terms

$$\sigma^{t,f} = \sigma^{t} \frac{\Gamma^{H\to f}}{\Gamma^{H}}$$

Linear model

EFT: Method

EFT impact on the cross-section of the truth bin t, decaying into final state f

$$\sigma^{t,f} = \boxed{\sigma^{t,f}_{SM}} + \boxed{\sigma^{t,f}_{int}} + \xcancel{\boxed{\sigma^{t,f}_{BSM}}}$$

Pure BSM contribution

Interference SM-BSM

Pure SM cross-section

Comparing:
Linear vs Linear + Quadratic
allows checking the possibility of neglecting dim 8 terms

$$\sigma^{t,f} = \sigma^{t} \frac{\Gamma^{H\to f}}{\Gamma^{H}}$$

Linear model

$$\mathcal{A}_k = \frac{\sigma_{int}}{\sigma_{SM}}$$

$$\mu_t^f \equiv \frac{\sigma_{t\ (int)}^{f}}{\sigma_{t\ (SM)}^{f}} = 1 + \sum_k \left[\mathcal{A}_k^{t\to H} + \mathcal{A}_k^{\Gamma_{H\to f}} - \mathcal{A}_k^{\Gamma_H^{total}}\right]\mathcal{C}_k$$

EFT: Method

EFT impact on the cross-section of the truth bin t, decaying into final state f

$$\sigma^{t,f} = \boxed{\sigma^{t,f}_{SM}} + \boxed{\sigma^{t,f}_{int}} + \cancel{\boxed{\sigma^{t,f}_{BSM}}}$$

Pure BSM contribution

Interference SM-BSM

Pure SM cross-section

Comparing:
Linear vs Linear + Quadratic
allows checking the possibility of neglecting dim 8 terms

$$\sigma^{t,f} = \boxed{\sigma^{t}}\frac{\Gamma^{H\to f}}{\Gamma^{H}}$$

Linear model

$$\mathcal{A}_k = \frac{\sigma_{int}}{\sigma_{SM}}$$

$$\mu_t^f \equiv \frac{\sigma^f_{t\ (int)}}{\sigma^f_{t\ (SM)}} = 1 + \sum_k \left[\boxed{\mathcal{A}_k^{t\to H}} + \boxed{\mathcal{A}_k^{\Gamma_{H\to f}} - \mathcal{A}_k^{\Gamma_H^{total}}}\right]\mathcal{C}_k$$

Depend only on the decay channel

Depend only on the production mode

Narrow width approximation:
no propagator correction

EFT: Method

EFT impact on the cross-section of the truth bin t, decaying into final state f

$$\sigma^{t,f} = \boxed{\sigma^{t,f}_{SM}} + \boxed{\sigma^{t,f}_{int}} + \cancel{\sigma^{t,f}_{BSM}}$$

Pure BSM contribution

Interference SM-BSM

Pure SM cross-section

Comparing:
Linear vs Linear + Quadratic
allows checking the possibility of neglecting dim 8 terms

$$\sigma^{t,f} = \boxed{\sigma^{t}} \frac{\boxed{\Gamma^{H\to f}}}{\boxed{\Gamma^{H}}}$$

Linear model

$$\mu^{f}_{t} \equiv \frac{\sigma^{f}_{t\ (int)}}{\sigma^{f}_{t\ (SM)}} = 1 + \sum_{k} \left[\boxed{\mathcal{A}_k^{t\to H}} + \boxed{\mathcal{A}_k^{\Gamma_{H\to f}} - \mathcal{A}_k^{\Gamma_H^{total}}} \right] \mathcal{C}_k$$

$$\mathcal{A}_k = \frac{\sigma_{int}}{\sigma_{SM}}$$

Depend only on the decay channel

Depend only on the production mode

Narrow width approximation:
no propagator correction

EFT interpretation: impact of coeffs on observables

Ratio to the SM xs

For various groups of operators

Visualisation: **impact** on the **production XS** and the **decay width** by each Wilson Coefficient

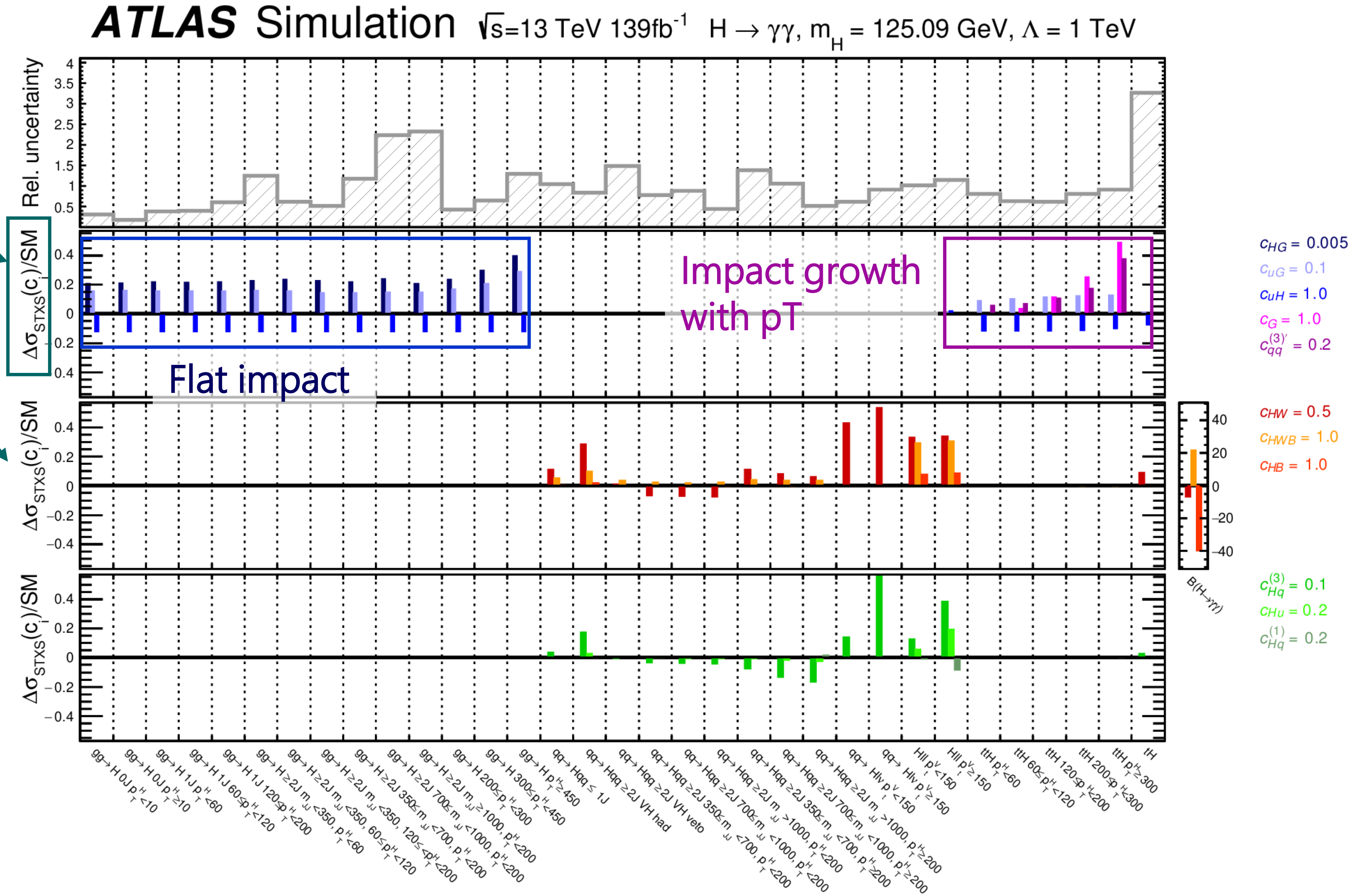

EFT interpretation: results, individual Ci

Measured values and 68% (95%) CI for the linear only and linear + quadratic parametrisations

One-at-time scan: float only one WC, others set to zero (SM value)

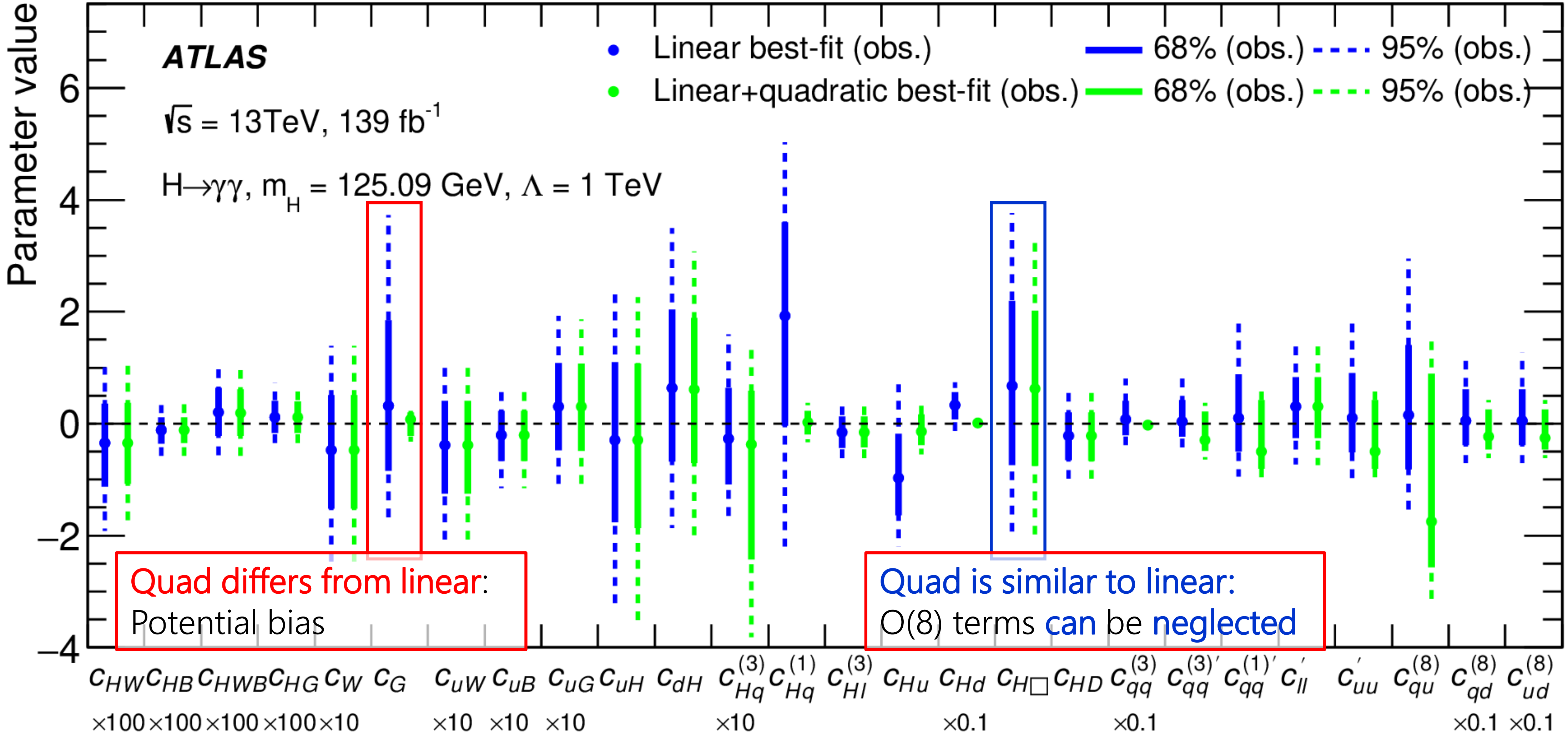

Quad differs from linear: Potential bias

Quad is similar to linear: O(8) terms can be neglected

EFT interpretation: PCA definition

Try to perform measurements of the most sensitive directions (PCA)

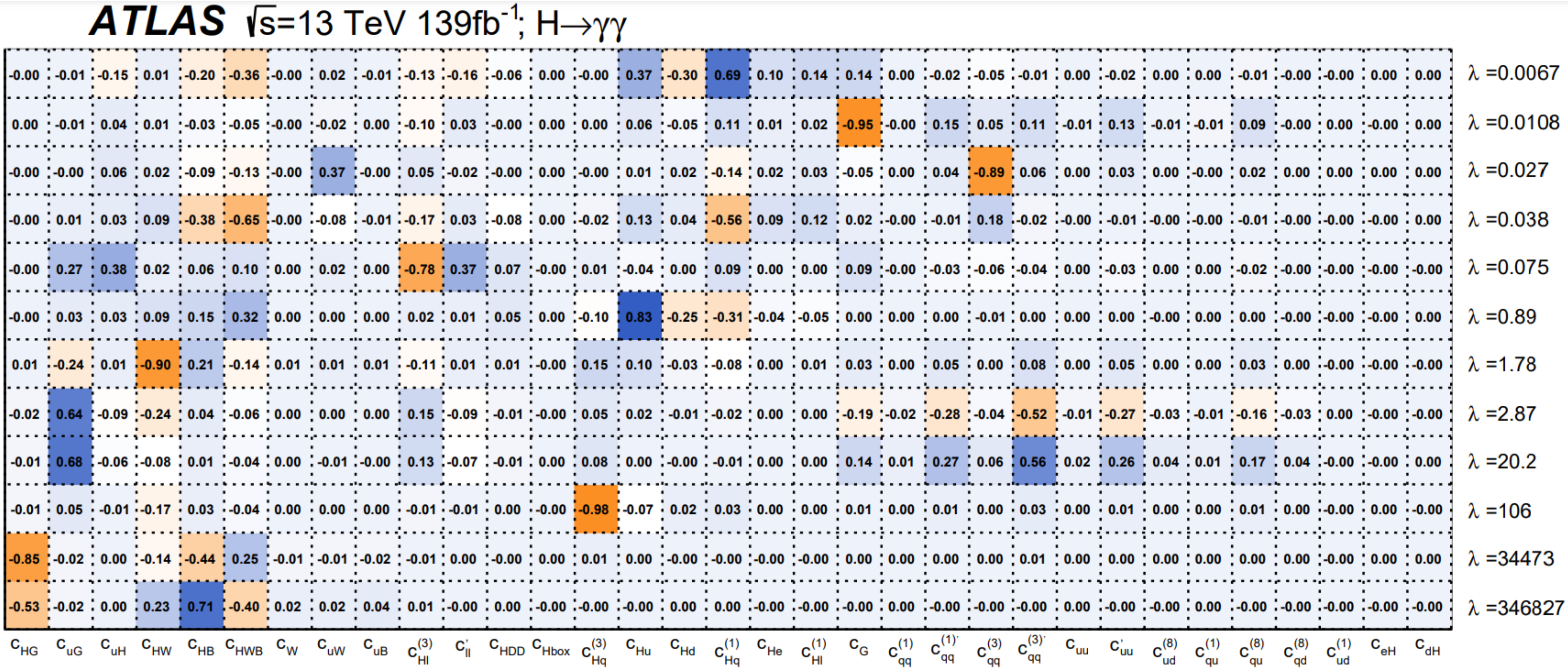

ATLAS $\sqrt{s}$=13 TeV 139fb^{-1}; H→γγ

	C_{HG}	C_{uG}	C_{uH}	C_{HW}	C_{HB}	C_{HWB}	C_{W}	C_{uW}	C_{uB}	$C_{Hl}^{(3)}$	C'_{ll}	C_{HDD}	C_{Hbox}	$C_{Hq}^{(3)}$	C_{Hu}	C_{Hd}	$C_{Hq}^{(1)}$	C_{He}	$C_{Hl}^{(1)}$	C_{G}	$C_{qq}^{(1)}$	$C_{qq}^{(1)'}$	$C_{qq}^{(3)}$	$C_{qq}^{(3)'}$	C_{uu}	C'_{uu}	$C_{ud}^{(8)}$	$C_{qu}^{(1)}$	$C_{qu}^{(8)}$	$C_{qd}^{(8)}$	$C_{ud}^{(1)}$	C_{eH}	C_{dH}	
EV12	-0.00	-0.01	-0.15	0.01	-0.20	-0.36	-0.00	0.02	-0.01	-0.13	-0.16	-0.06	0.00	-0.00	0.37	-0.30	0.69	0.10	0.14	0.14	0.00	-0.02	-0.05	-0.01	0.00	-0.02	0.00	0.00	-0.01	-0.00	-0.00	0.00	0.00	λ =0.0067
EV11	0.00	-0.01	0.04	0.01	-0.03	-0.05	-0.00	-0.02	0.00	-0.10	0.03	-0.00	0.00	0.00	0.06	-0.05	0.11	0.01	0.02	-0.95	-0.00	0.15	0.05	0.11	-0.01	0.13	-0.01	-0.01	0.09	-0.00	0.00	-0.00	0.00	λ =0.0108
EV10	-0.00	-0.00	0.06	0.02	-0.09	-0.13	-0.00	0.37	-0.00	0.05	-0.02	-0.00	0.00	-0.00	0.01	0.02	-0.14	0.02	0.03	-0.05	0.00	0.04	-0.89	0.06	0.00	0.03	0.00	-0.00	0.02	0.00	0.00	0.00	0.00	λ =0.027
EV9	-0.00	0.01	0.03	0.09	-0.38	-0.65	-0.00	-0.08	-0.01	-0.17	0.03	-0.08	0.00	-0.02	0.13	0.04	-0.56	0.09	0.12	0.02	-0.00	-0.01	0.18	-0.02	-0.00	-0.01	-0.00	-0.00	-0.01	-0.00	-0.00	-0.00	0.00	λ =0.038
EV8	-0.00	0.27	0.38	0.02	0.06	0.10	0.00	0.02	0.00	-0.78	0.37	0.07	-0.00	0.01	-0.04	0.00	0.09	0.00	0.00	0.09	-0.00	-0.03	-0.06	-0.04	0.00	-0.03	0.00	0.00	-0.02	-0.00	-0.00	-0.00	-0.00	λ =0.075
EV7	-0.00	0.03	0.03	0.09	0.15	0.32	0.00	0.00	0.00	0.02	0.01	0.05	0.00	-0.10	0.83	-0.25	-0.31	-0.04	-0.05	0.00	0.00	0.00	-0.01	0.00	0.00	0.00	-0.00	0.00	0.00	-0.00	-0.00	-0.00	0.00	λ =0.89
EV6	0.01	-0.24	0.01	-0.90	0.21	-0.14	0.01	0.01	0.01	-0.11	0.01	0.01	-0.00	0.15	0.10	-0.03	-0.08	0.00	0.01	0.03	0.00	0.05	0.00	0.08	0.00	0.05	0.00	0.00	0.03	0.00	-0.00	-0.00	-0.00	λ =1.78
EV5	-0.02	0.64	-0.09	-0.24	0.04	-0.06	0.00	0.00	0.00	0.15	-0.09	-0.01	-0.00	0.05	0.02	-0.01	-0.02	0.00	0.00	-0.19	-0.02	-0.28	-0.04	-0.52	-0.01	-0.27	-0.03	-0.01	-0.16	-0.03	0.00	-0.00	-0.00	λ =2.87
EV4	-0.01	0.68	-0.06	-0.08	0.01	-0.04	0.00	-0.01	-0.00	0.13	-0.07	-0.01	0.00	0.08	0.00	-0.00	-0.01	0.00	0.00	0.14	0.01	0.27	0.06	0.56	0.02	0.26	0.04	0.01	0.17	0.04	-0.00	-0.00	0.00	λ =20.2
EV3	-0.01	0.05	-0.01	-0.17	0.03	-0.04	0.00	0.00	0.00	-0.01	-0.01	0.00	-0.00	-0.98	-0.07	0.02	0.03	0.00	0.00	0.01	0.00	0.01	0.00	0.03	0.00	0.01	0.00	0.00	0.01	0.00	-0.00	0.00	-0.00	λ =106
EV2	-0.85	-0.02	0.00	-0.14	-0.44	0.25	-0.01	-0.01	-0.02	-0.01	0.00	-0.00	0.00	0.01	0.00	-0.00	-0.00	-0.00	-0.00	0.00	0.00	0.00	0.00	0.01	0.00	0.00	0.00	0.00	0.00	0.00	-0.00	0.00	0.00	λ =34473
EV1	-0.53	-0.02	0.00	0.23	0.71	-0.40	0.02	0.02	0.04	0.01	-0.00	0.00	-0.00	-0.00	-0.00	0.00	0.00	-0.00	-0.00	-0.00	0.00	-0.00	-0.00	-0.00	0.00	-0.00	-0.00	0.00	-0.00	-0.00	-0.00	-0.00	-0.00	λ =346827

EFT interpretation: PCA results

Simultaneous fit over 12 eigen-vectors

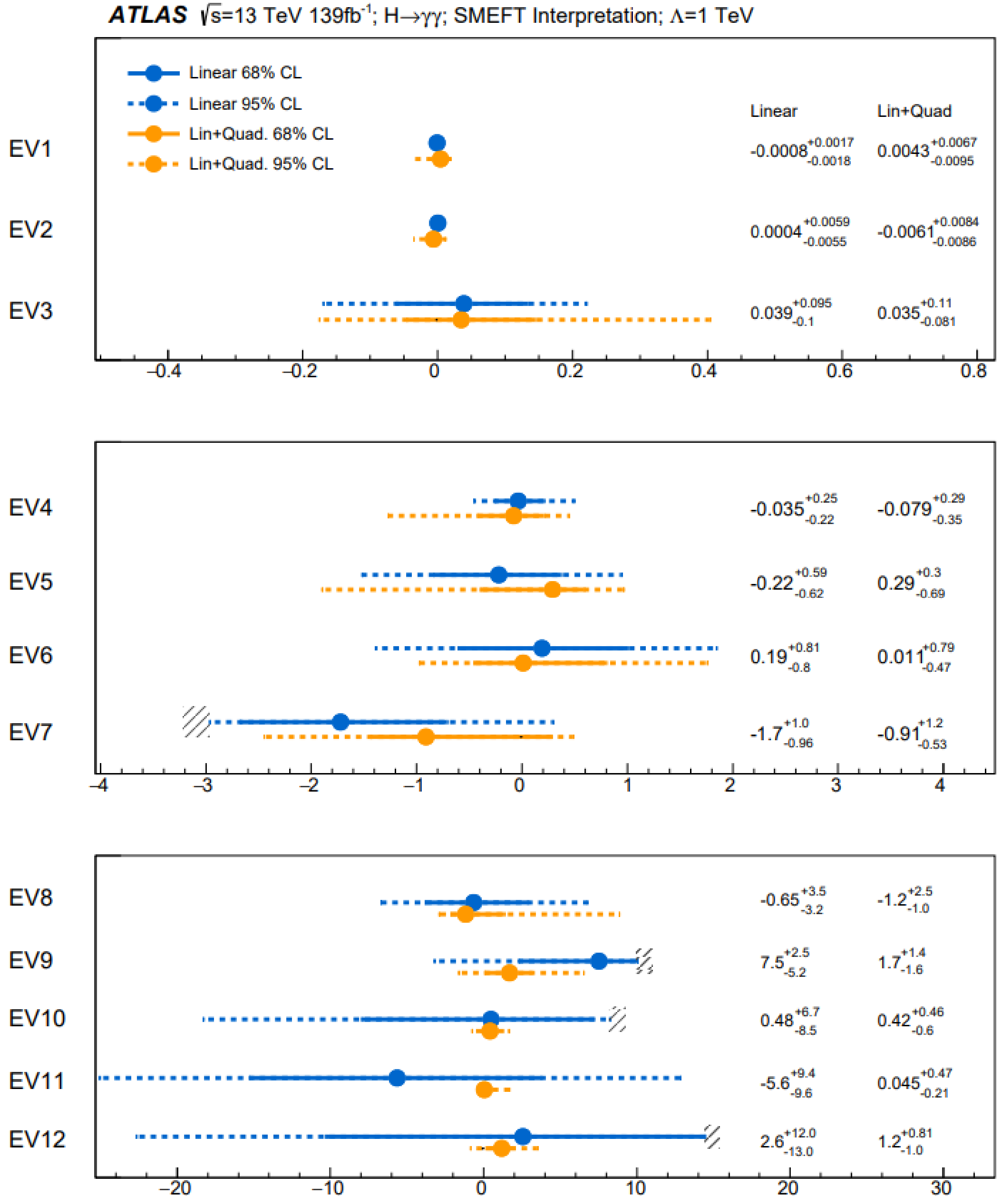

Likelihood scans

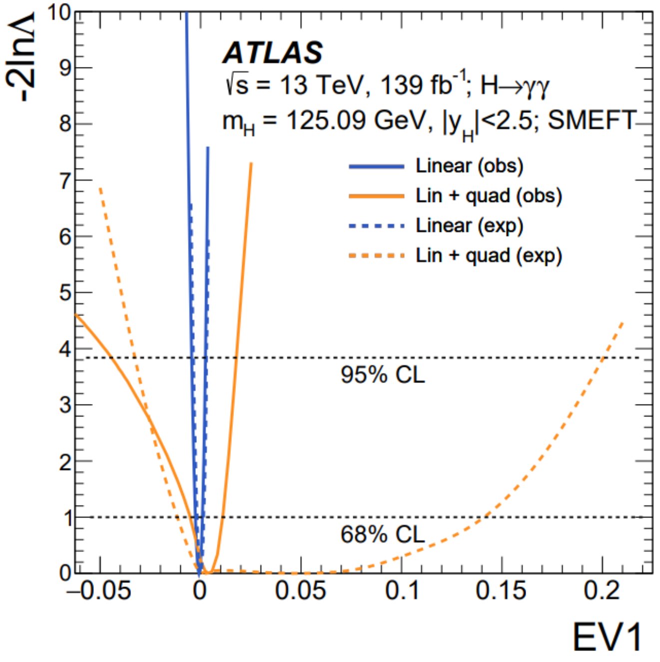

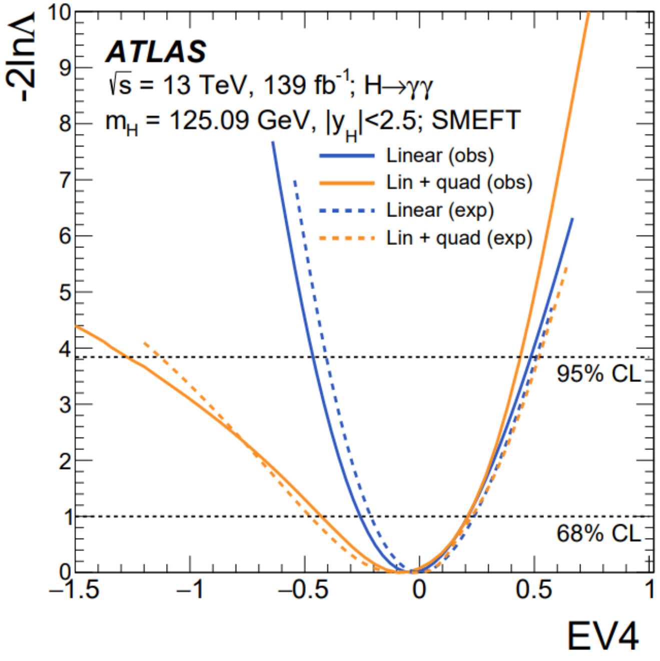

EFT interpretation: combination of channels

Channels considered in the combination:

ATLAS-CONF-2021-053

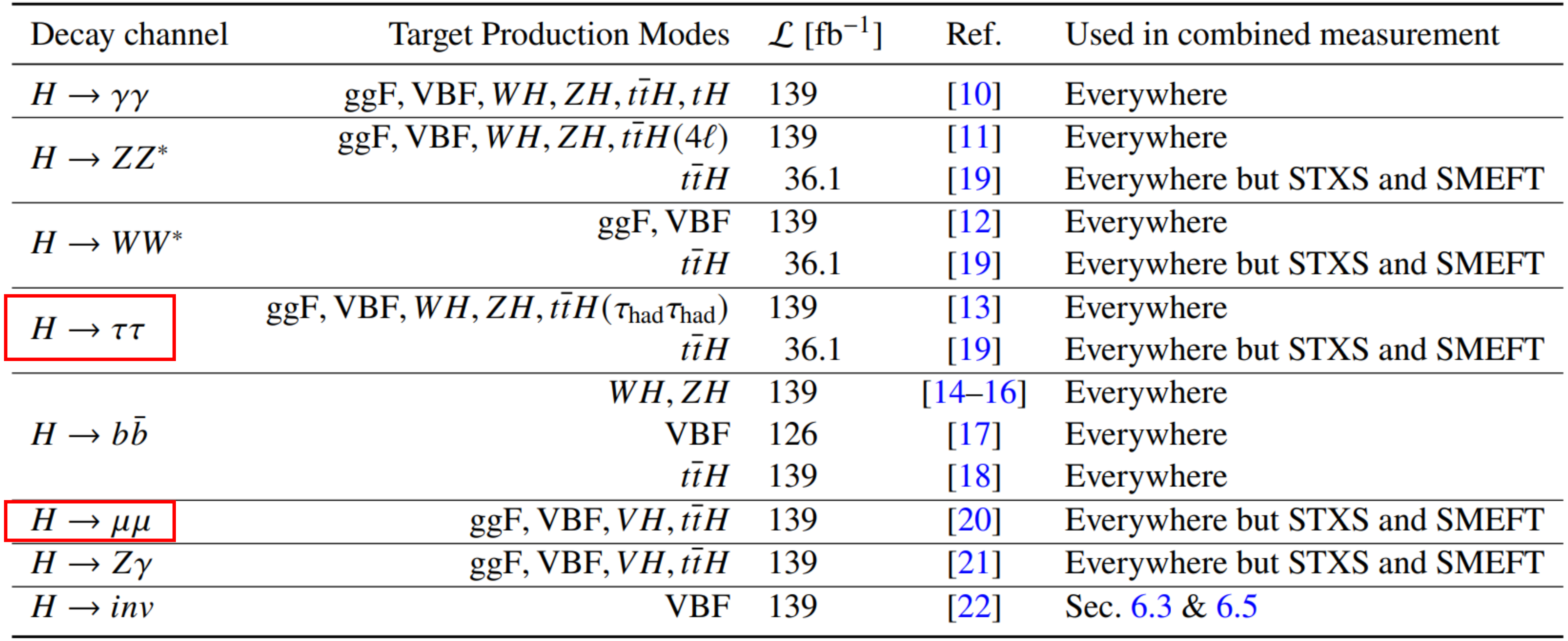

Decay channel	Target Production Modes	$\mathcal{L}$ [fb^{-1}]	Ref.	Used in combined measurement
$H \to \gamma\gamma$	ggF, VBF, $WH, ZH, t\bar{t}H, tH$	139	[10]	Everywhere
$H \to ZZ^*$	ggF, VBF, $WH, ZH, t\bar{t}H(4\ell)$	139	[11]	Everywhere
	$t\bar{t}H$	36.1	[19]	Everywhere but STXS and SMEFT
$H \to WW^*$	ggF, VBF	139	[12]	Everywhere
	$t\bar{t}H$	36.1	[19]	Everywhere but STXS and SMEFT
$H \to \tau\tau$	ggF, VBF, $WH, ZH, t\bar{t}H(\tau_{\mathrm{had}}\tau_{\mathrm{had}})$	139	[13]	Everywhere
	$t\bar{t}H$	36.1	[19]	Everywhere but STXS and SMEFT
$H \to b\bar{b}$	WH, ZH	139	[14–16]	Everywhere
	VBF	126	[17]	Everywhere
	$t\bar{t}H$	139	[18]	Everywhere
$H \to \mu\mu$	ggF, VBF, $VH, t\bar{t}H$	139	[20]	Everywhere but STXS and SMEFT
$H \to Z\gamma$	ggF, VBF, $VH, t\bar{t}H$	139	[21]	Everywhere but STXS and SMEFT
$H \to inv$	VBF	139	[22]	Sec. 6.3 & 6.5

$(cc), (\tau\tau), (\mu\mu)$ Channels are not included due to the underlying topU3l symmetry:

- Leptons between generations are not distinguished
- 2nd generation quarks are not distinguished

EFT interpretation: combined measurements

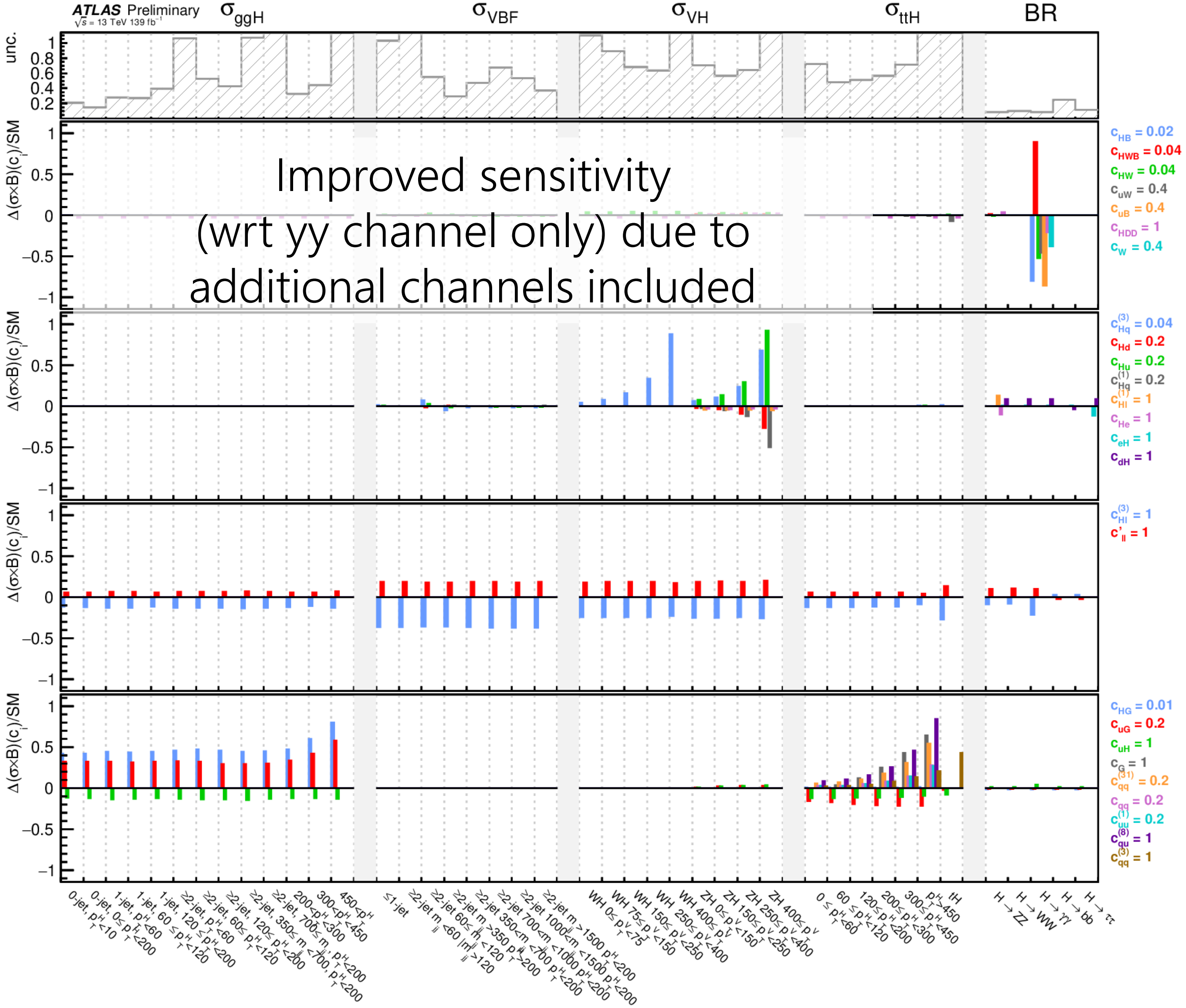

Improved sensitivity (wrt yy channel only) due to additional channels included

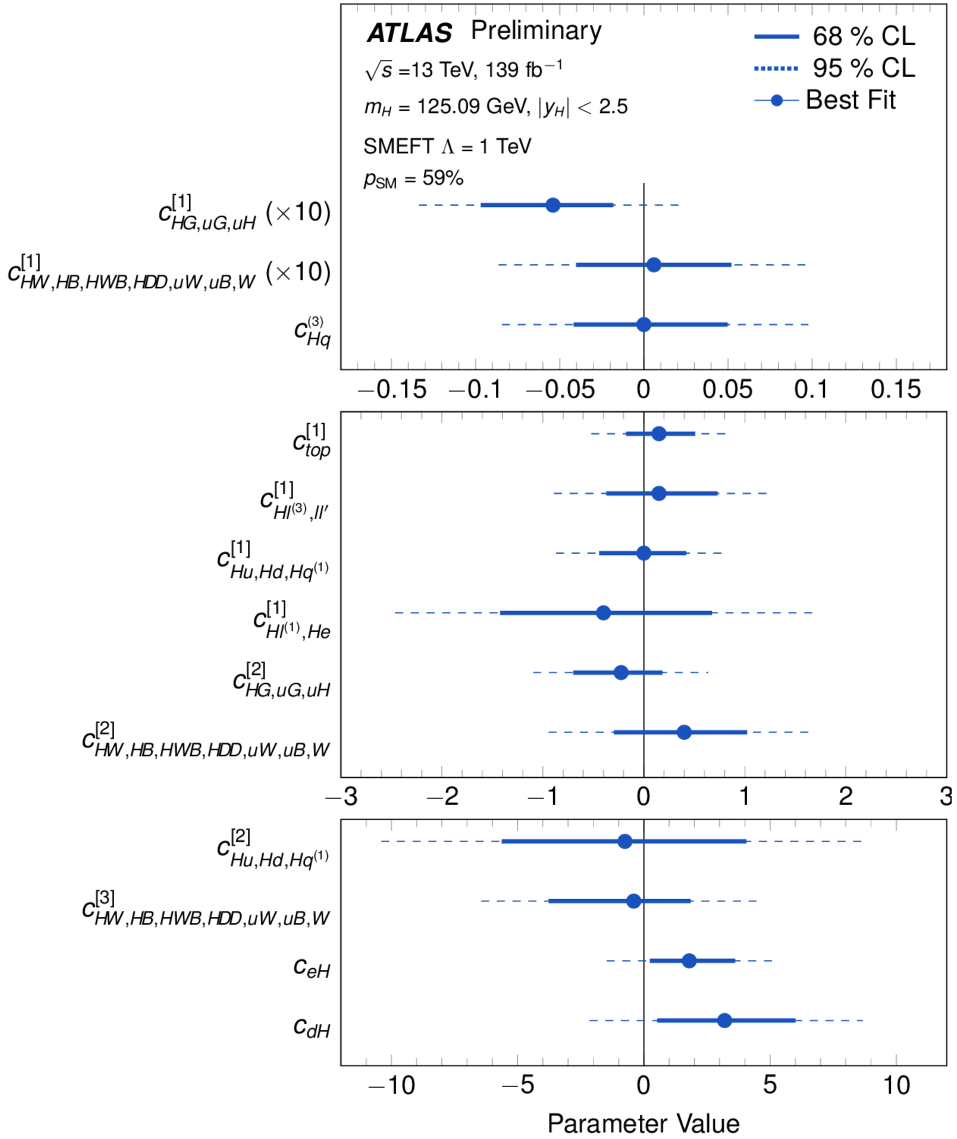

Conclusion

- Diphoton channel allows precise measurements in the Higgs sector
- STXS framework: suitable for combination
- Measurements: inclusive, production modes, STXS, kappa-framework
- EFT interpretation in the SMEFT

Prospects

- EFT interpretation of combined Higgs measurements

Contributions

Signal & background modelling. Spurious signal evaluation.
Acceptances, purities, estimation.
Likelihood scans, sensitivities.
Ongoing activity on the combined EFT fits.

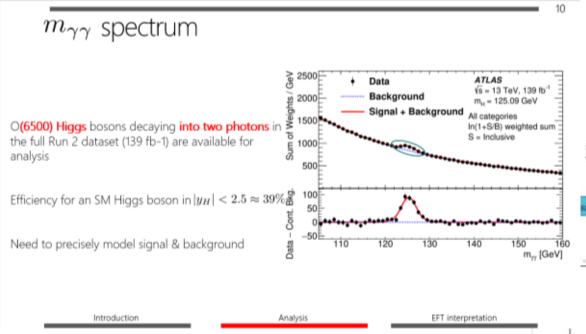

10

$m_{\gamma\gamma}$ spectrum

O(6500) Higgs bosons decaying into two photons in the full Run 2 dataset (139 fb-1) are available for analysis

Efficiency for an SM Higgs boson in $|y_H| < 2.5 \approx 39\%$

Need to precisely model signal & background

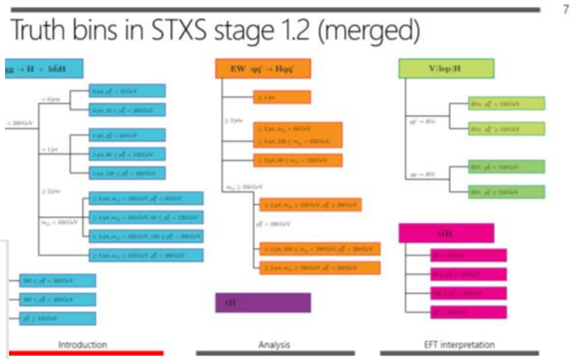

7

Truth bins in STXS stage 1.2 (merged)

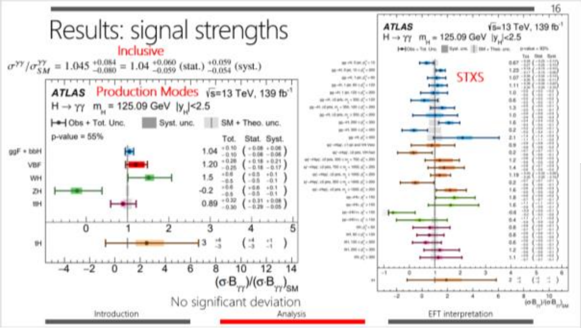

16

Results: signal strengths

Inclusive

$\sigma^{\gamma\gamma}/\sigma^{\gamma\gamma}_{SM} = 1.045^{+0.084}_{-0.080} = 1.04^{+0.060}_{-0.059}\text{ (stat.) }^{+0.059}_{-0.054}\text{ (syst.)}$

Production Modes

STXS

No significant deviation

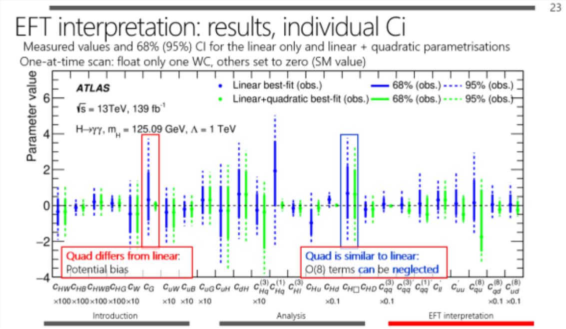

23

EFT interpretation: results, individual Ci

Measured values and 68% (95%) CI for the linear only and linear + quadratic parametrisations

One-at-time scan: float only one WC, others set to zero (SM value)

Quad differs from linear: Potential bias

Quad is similar to linear: O(8) terms can be neglected

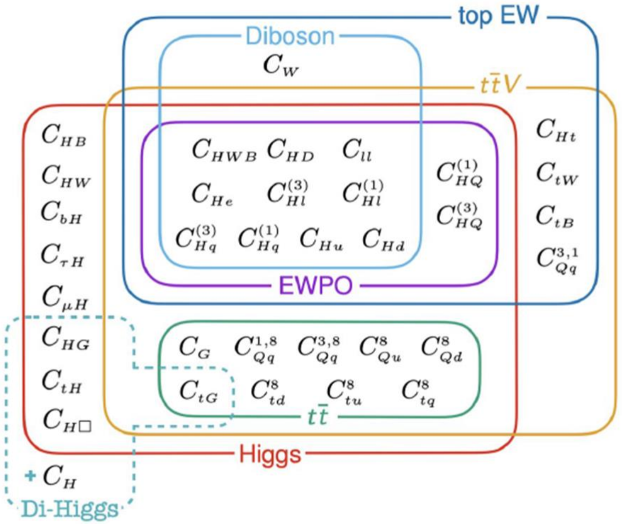

Back-up

EFT interpretation: Symmetry scheme

topU3l: scheme used in ATLAS global combination

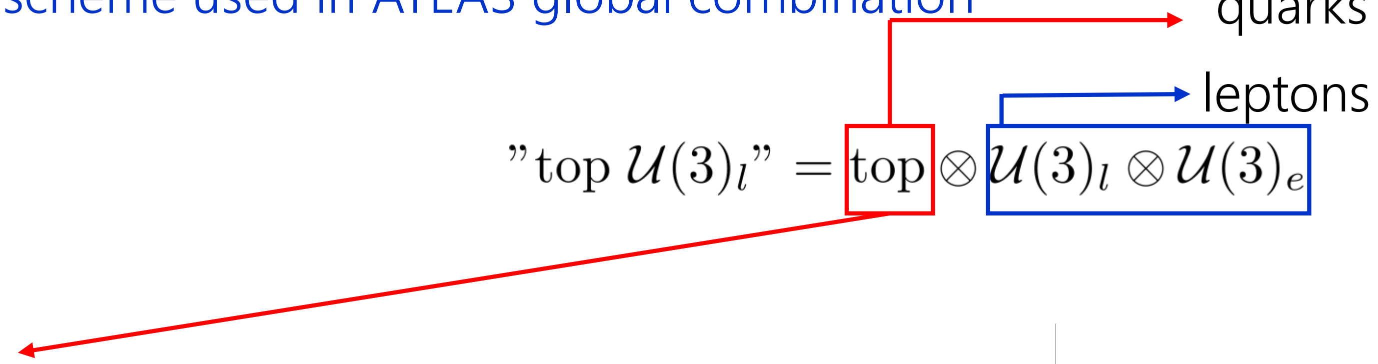

$$\text{"top } \mathcal{U}(3)_l\text{"} = \boxed{\text{top}} \otimes \boxed{\mathcal{U}(3)_l \otimes \mathcal{U}(3)_e}$$

Quarks:

1st + 2nd generations:

$$(q_l, u_r, d_r) \in \mathcal{U}(2)_q \otimes \mathcal{U}(2)_u \otimes \mathcal{U}(2)_d$$

3rd generation:

$$(Q_L, t_r, b_r) \text{ - no symmetry}$$

no CKM

$$\mathbb{V}_{CKM} = \mathbb{1}$$

“At energy scales, where the first two generations of quarks are undistinguishable”

EFT interpretation: Symmetry scheme

topU3l: scheme used in ATLAS global combination

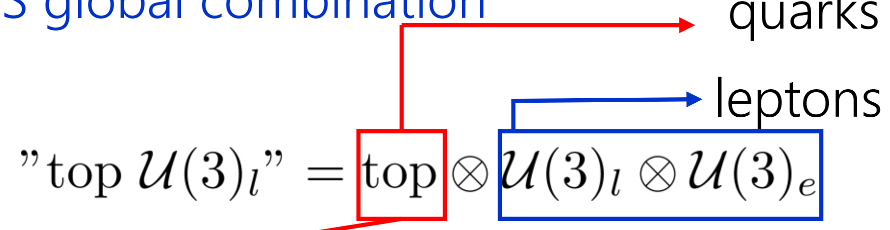

$$\text{"top } \mathcal{U}(3)_l\text{"} = \boxed{\text{top}} \otimes \boxed{\mathcal{U}(3)_l \otimes \mathcal{U}(3)_e}$$

Quarks:

1st + 2nd generations:

$$(q_l, u_r, d_r) \in \mathcal{U}(2)_q \otimes \mathcal{U}(2)_u \otimes \mathcal{U}(2)_d$$

3rd generation:

$$(Q_L, t_r, b_r) \text{ - no symmetry}$$

no CKM

$$\mathbb{V}_{CKM} = \mathbb{1}$$

"At energy scales, where the first two generations of quarks are undistinguishable"

Leptons: $\mathcal{U}(3)_l = \mathcal{U}(3)_l \otimes \mathcal{U}(3)_e$

All generations symmetry:

$$e = \mu = \tau$$

No mixing

Input parameters:

$$(m_W, m_Z, G_F)$$

Luminosity @ Run 2

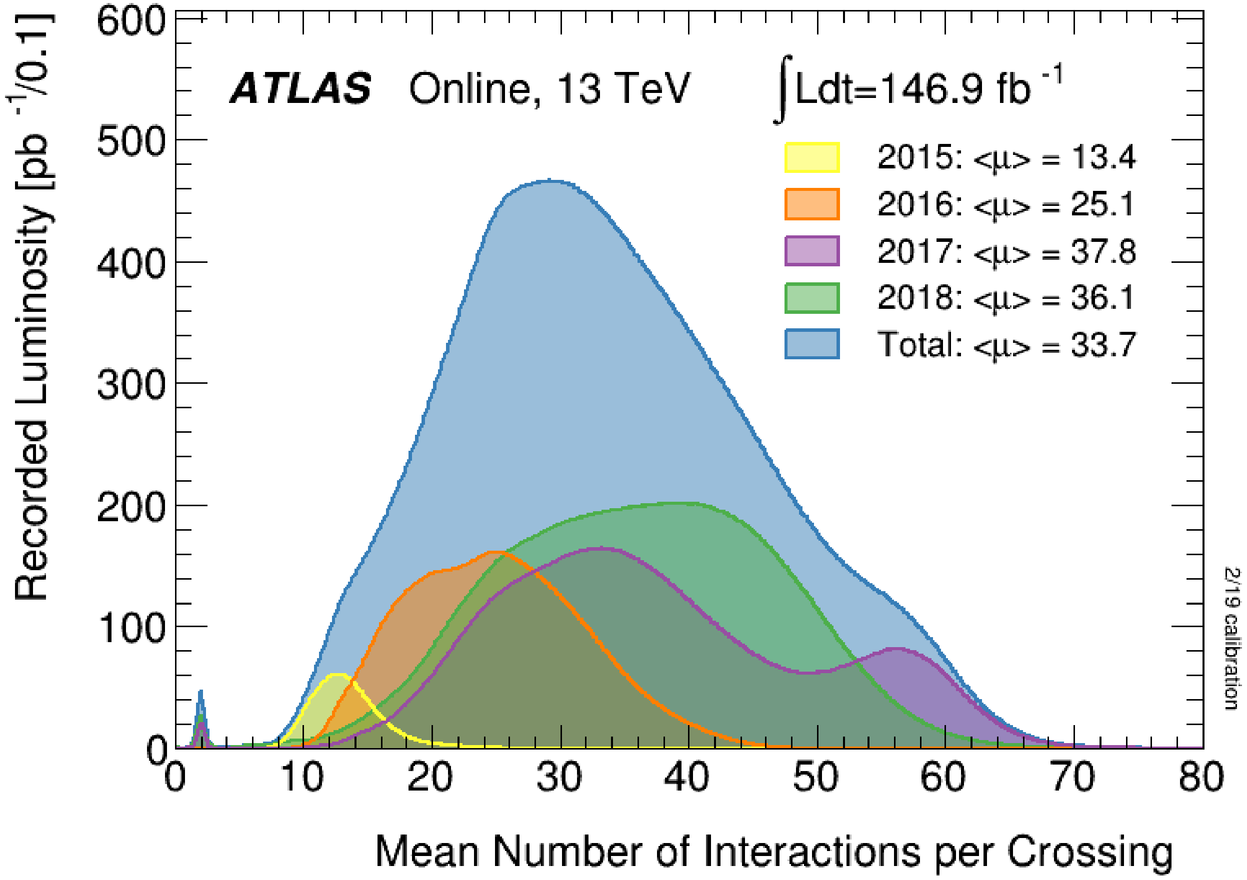

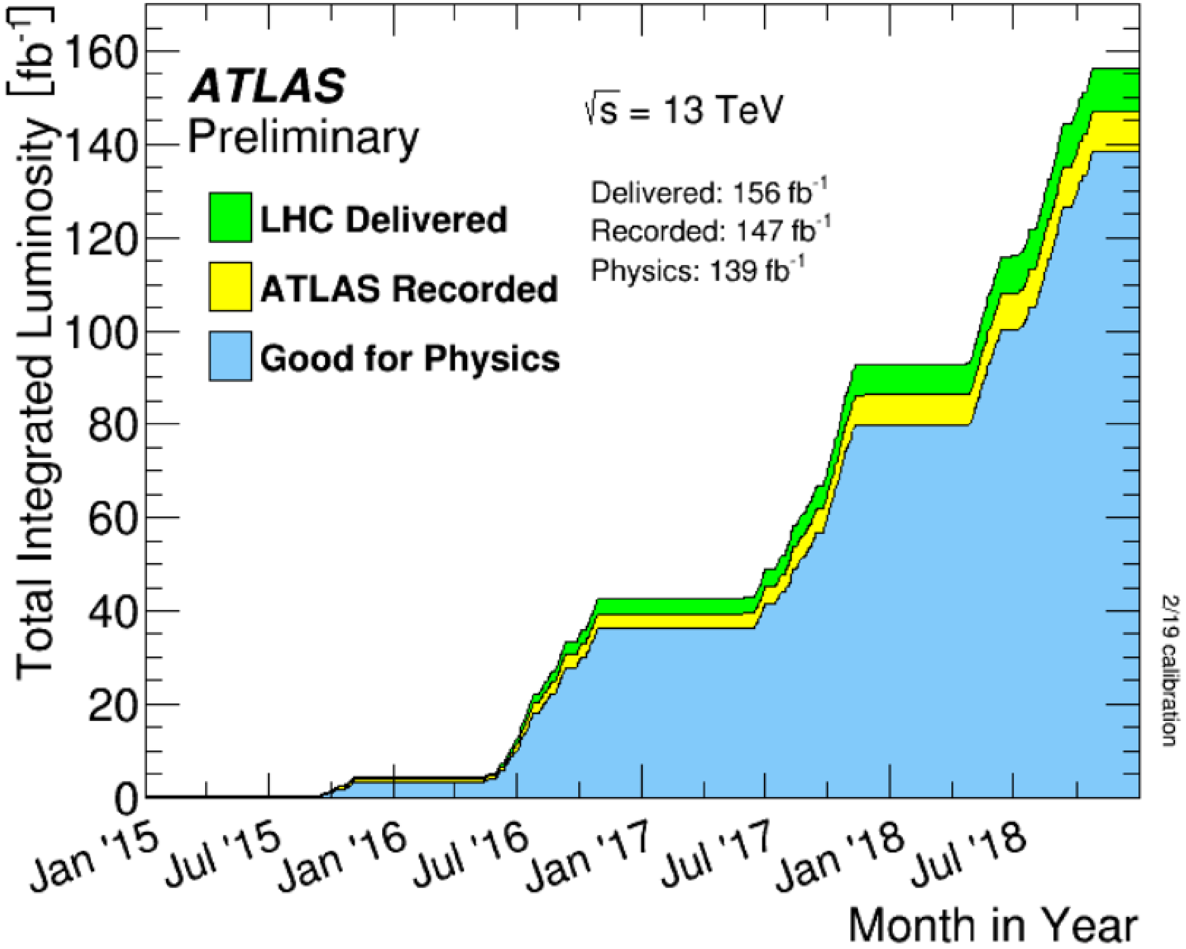

Double-sided Crystal-ball

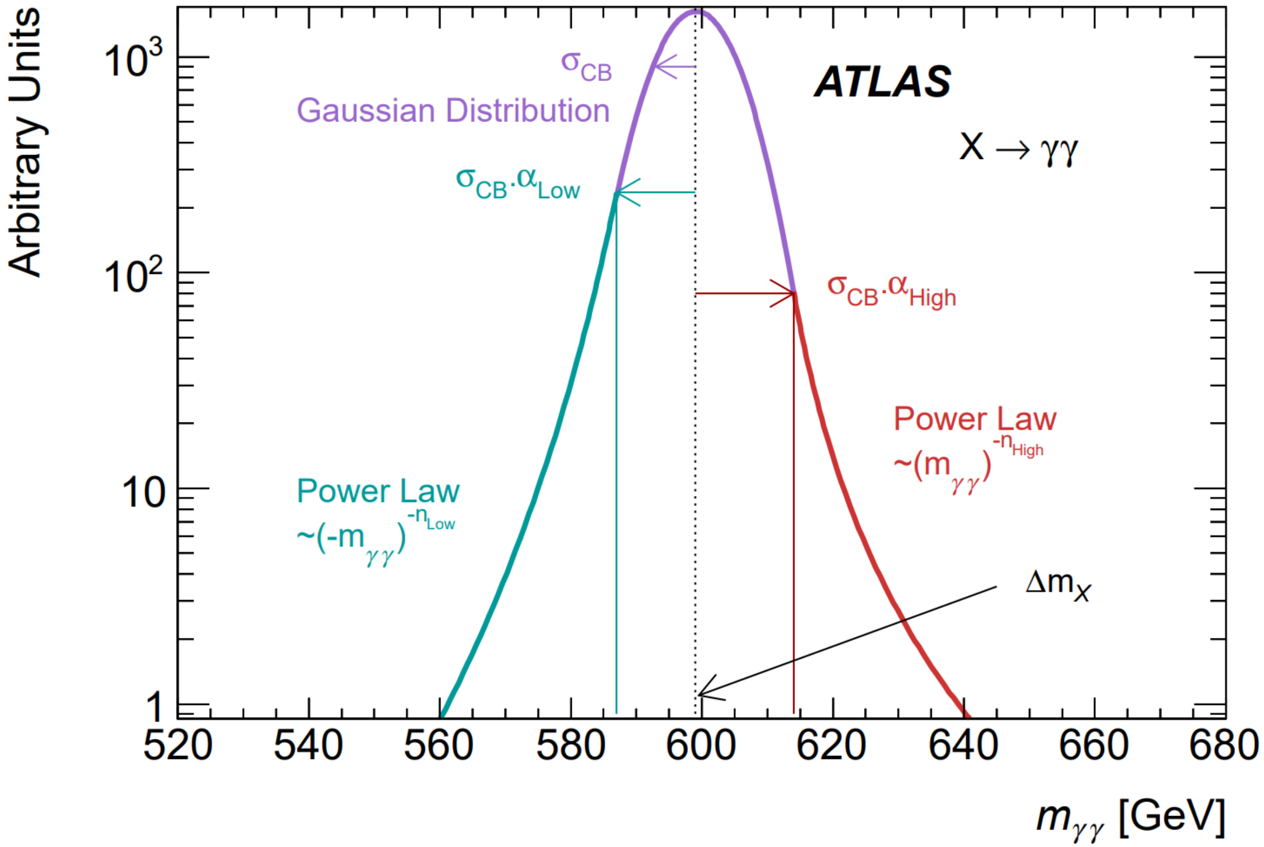

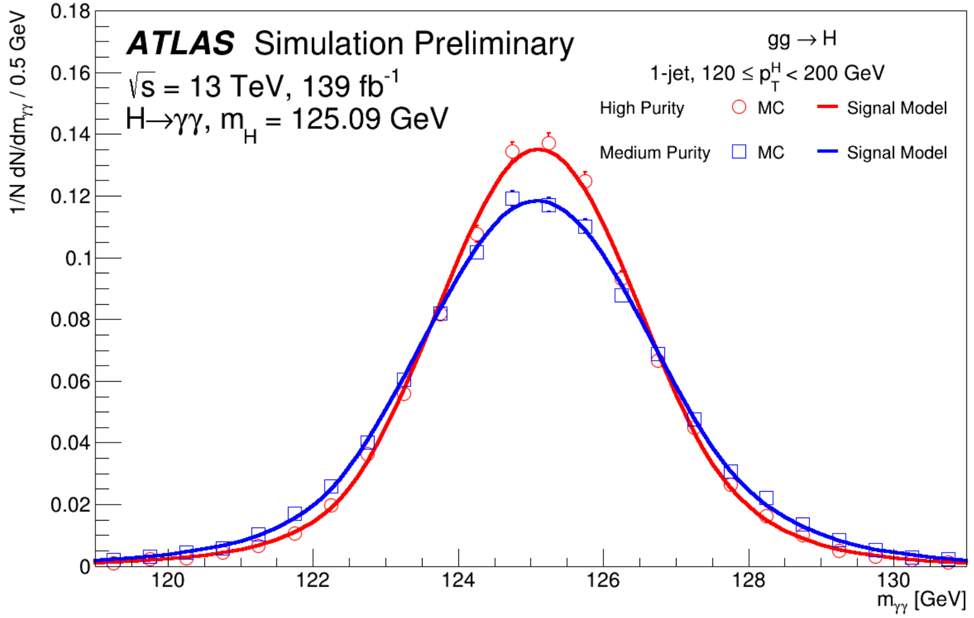

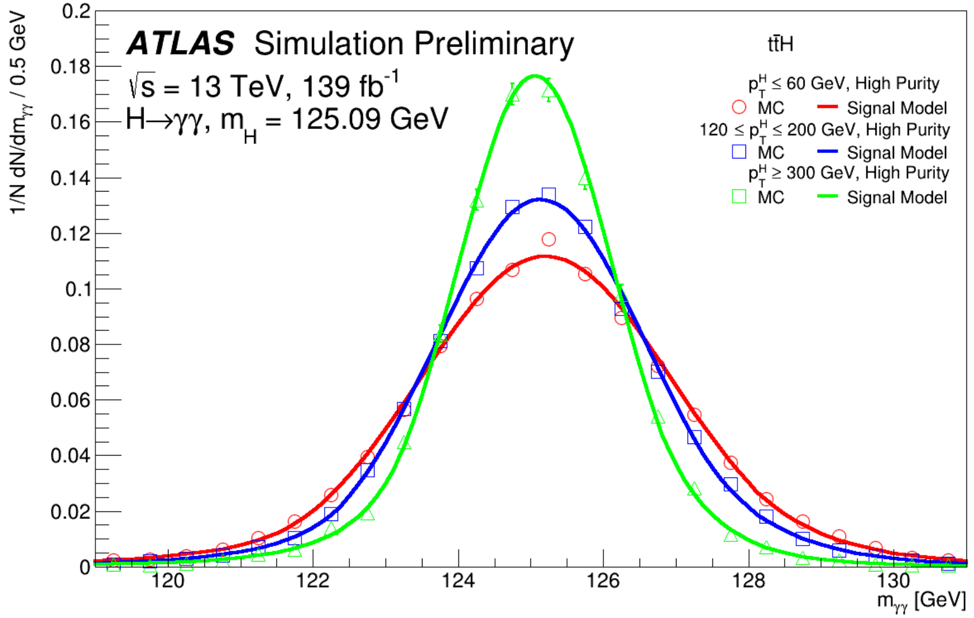

Table 10: Wilson coefficients c_i and corresponding dimension-6 SMEFT operators $O_i^{(6)}$ used in this analysis.

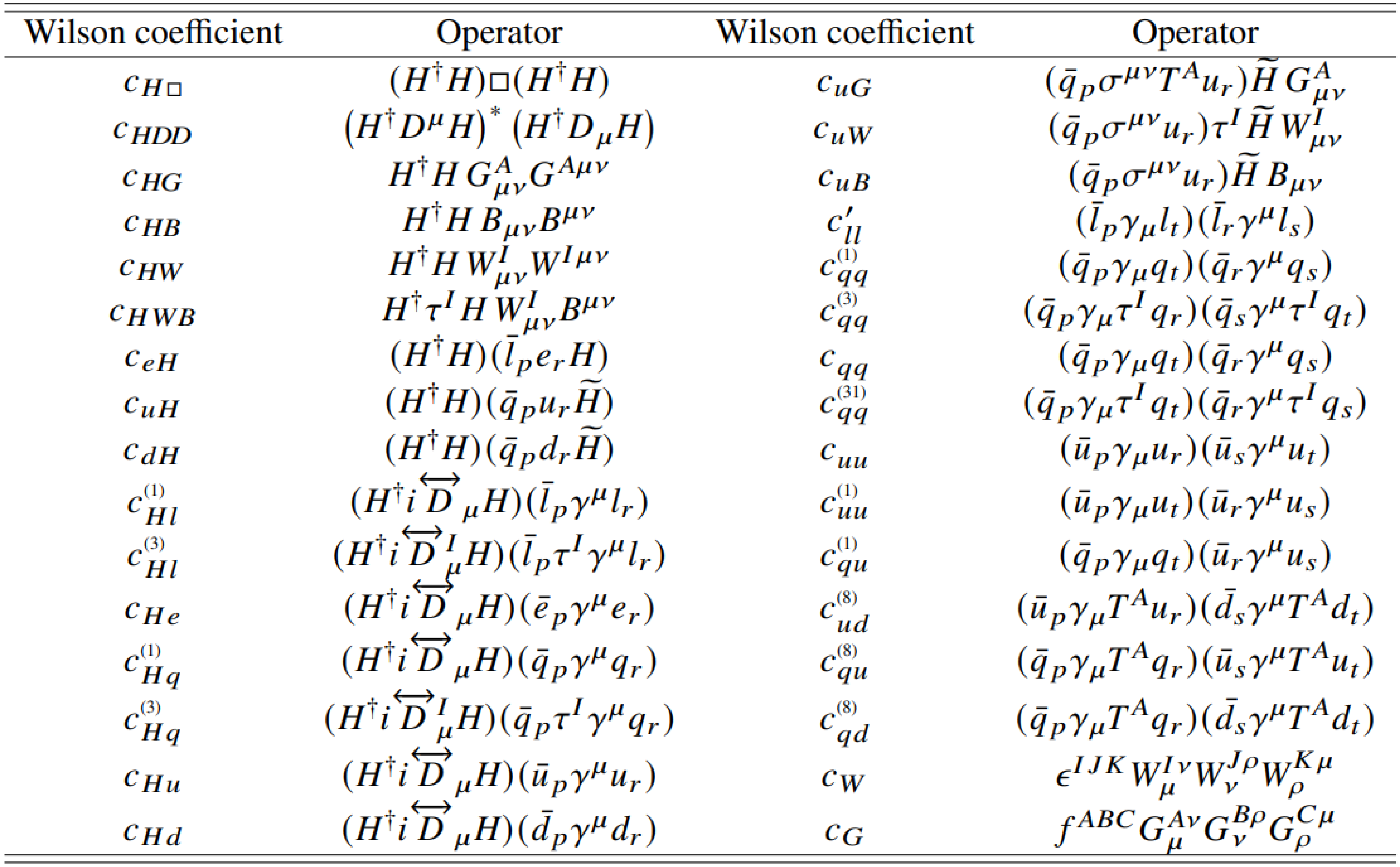

Wilson coefficient	Operator	Wilson coefficient	Operator
$c_{H\Box}$	$(H^\dagger H)\Box(H^\dagger H)$	c_{uG}	$(\bar{q}_p\sigma^{\mu\nu}T^A u_r)\widetilde{H}\, G^A_{\mu\nu}$
c_{HDD}	$\left(H^\dagger D^\mu H\right)^* \left(H^\dagger D_\mu H\right)$	c_{uW}	$(\bar{q}_p\sigma^{\mu\nu}u_r)\tau^I \widetilde{H}\, W^I_{\mu\nu}$
c_{HG}	$H^\dagger H\, G^A_{\mu\nu}G^{A\mu\nu}$	c_{uB}	$(\bar{q}_p\sigma^{\mu\nu}u_r)\widetilde{H}\, B_{\mu\nu}$
c_{HB}	$H^\dagger H\, B_{\mu\nu}B^{\mu\nu}$	c'_{ll}	$(\bar{l}_p\gamma_\mu l_t)(\bar{l}_r\gamma^\mu l_s)$
c_{HW}	$H^\dagger H\, W^I_{\mu\nu}W^{I\mu\nu}$	$c^{(1)}_{qq}$	$(\bar{q}_p\gamma_\mu q_t)(\bar{q}_r\gamma^\mu q_s)$
c_{HWB}	$H^\dagger\tau^I H\, W^I_{\mu\nu}B^{\mu\nu}$	$c^{(3)}_{qq}$	$(\bar{q}_p\gamma_\mu\tau^I q_r)(\bar{q}_s\gamma^\mu\tau^I q_t)$
c_{eH}	$(H^\dagger H)(\bar{l}_p e_r H)$	c_{qq}	$(\bar{q}_p\gamma_\mu q_t)(\bar{q}_r\gamma^\mu q_s)$
c_{uH}	$(H^\dagger H)(\bar{q}_p u_r\widetilde{H})$	$c^{(31)}_{qq}$	$(\bar{q}_p\gamma_\mu\tau^I q_t)(\bar{q}_r\gamma^\mu\tau^I q_s)$
c_{dH}	$(H^\dagger H)(\bar{q}_p d_r\widetilde{H})$	c_{uu}	$(\bar{u}_p\gamma_\mu u_r)(\bar{u}_s\gamma^\mu u_t)$
$c^{(1)}_{Hl}$	$(H^\dagger i\overleftrightarrow{D}_\mu H)(\bar{l}_p\gamma^\mu l_r)$	$c^{(1)}_{uu}$	$(\bar{u}_p\gamma_\mu u_t)(\bar{u}_r\gamma^\mu u_s)$
$c^{(3)}_{Hl}$	$(H^\dagger i\overleftrightarrow{D}^I_\mu H)(\bar{l}_p\tau^I\gamma^\mu l_r)$	$c^{(1)}_{qu}$	$(\bar{q}_p\gamma_\mu q_t)(\bar{u}_r\gamma^\mu u_s)$
c_{He}	$(H^\dagger i\overleftrightarrow{D}_\mu H)(\bar{e}_p\gamma^\mu e_r)$	$c^{(8)}_{ud}$	$(\bar{u}_p\gamma_\mu T^A u_r)(\bar{d}_s\gamma^\mu T^A d_t)$
$c^{(1)}_{Hq}$	$(H^\dagger i\overleftrightarrow{D}_\mu H)(\bar{q}_p\gamma^\mu q_r)$	$c^{(8)}_{qu}$	$(\bar{q}_p\gamma_\mu T^A q_r)(\bar{u}_s\gamma^\mu T^A u_t)$
$c^{(3)}_{Hq}$	$(H^\dagger i\overleftrightarrow{D}^I_\mu H)(\bar{q}_p\tau^I\gamma^\mu q_r)$	$c^{(8)}_{qd}$	$(\bar{q}_p\gamma_\mu T^A q_r)(\bar{d}_s\gamma^\mu T^A d_t)$
c_{Hu}	$(H^\dagger i\overleftrightarrow{D}_\mu H)(\bar{u}_p\gamma^\mu u_r)$	c_W	$\epsilon^{IJK}W^{I\nu}_\mu W^{J\rho}_\nu W^{K\mu}_\rho$
c_{Hd}	$(H^\dagger i\overleftrightarrow{D}_\mu H)(\bar{d}_p\gamma^\mu d_r)$	c_G	$f^{ABC}G^{A\nu}_\mu G^{B\rho}_\nu G^{C\mu}_\rho$

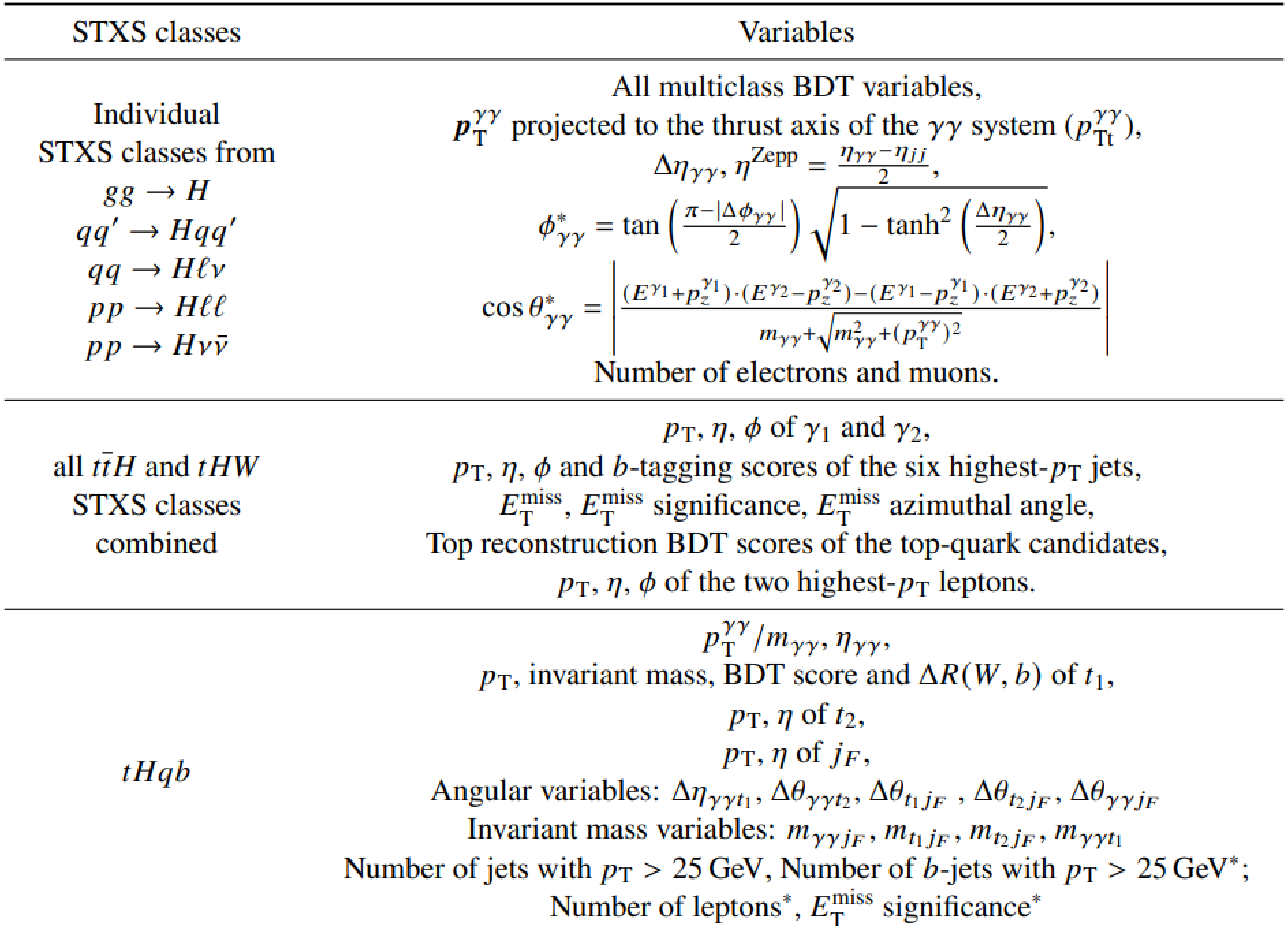

STXS classes	Variables
Individual STXS classes from $gg \to H$ $qq' \to Hqq'$ $qq \to H\ell\nu$ $pp \to H\ell\ell$ $pp \to H\nu\bar{\nu}$	All multiclass BDT variables, $\boldsymbol{p}_{\mathrm{T}}^{\gamma\gamma}$ projected to the thrust axis of the $\gamma\gamma$ system ($p_{\mathrm{Tt}}^{\gamma\gamma}$), $\Delta\eta_{\gamma\gamma}$, $\eta^{\mathrm{Zepp}} = \frac{\eta_{\gamma\gamma}-\eta_{jj}}{2}$, $\phi^*_{\gamma\gamma} = \tan\left(\frac{\pi-\lvert\Delta\phi_{\gamma\gamma}\rvert}{2}\right)\sqrt{1-\tanh^2\left(\frac{\Delta\eta_{\gamma\gamma}}{2}\right)}$, $\cos\theta^*_{\gamma\gamma} = \left\lvert\frac{(E^{\gamma_1}+p_z^{\gamma_1})\cdot(E^{\gamma_2}-p_z^{\gamma_2})-(E^{\gamma_1}-p_z^{\gamma_1})\cdot(E^{\gamma_2}+p_z^{\gamma_2})}{m_{\gamma\gamma}+\sqrt{m_{\gamma\gamma}^2+(p_{\mathrm{T}}^{\gamma\gamma})^2}}\right\rvert$ Number of electrons and muons.
all $t\bar{t}H$ and tHW STXS classes combined	p_{T}, η, ϕ of γ_1 and γ_2, p_{T}, η, ϕ and b-tagging scores of the six highest-p_{T} jets, $E_{\mathrm{T}}^{\mathrm{miss}}$, $E_{\mathrm{T}}^{\mathrm{miss}}$ significance, $E_{\mathrm{T}}^{\mathrm{miss}}$ azimuthal angle, Top reconstruction BDT scores of the top-quark candidates, p_{T}, η, ϕ of the two highest-p_{T} leptons.
$tHqb$	$p_{\mathrm{T}}^{\gamma\gamma}/m_{\gamma\gamma}$, $\eta_{\gamma\gamma}$, p_{T}, invariant mass, BDT score and $\Delta R(W,b)$ of t_1, p_{T}, η of t_2, p_{T}, η of j_F, Angular variables: $\Delta\eta_{\gamma\gamma t_1}$, $\Delta\theta_{\gamma\gamma t_2}$, $\Delta\theta_{t_1 j_F}$, $\Delta\theta_{t_2 j_F}$, $\Delta\theta_{\gamma\gamma j_F}$ Invariant mass variables: $m_{\gamma\gamma j_F}$, $m_{t_1 j_F}$, $m_{t_2 j_F}$, $m_{\gamma\gamma t_1}$ Number of jets with $p_{\mathrm{T}} > 25\,\mathrm{GeV}$, Number of b-jets with $p_{\mathrm{T}} > 25\,\mathrm{GeV}^*$; Number of leptons*, $E_{\mathrm{T}}^{\mathrm{miss}}$ significance*

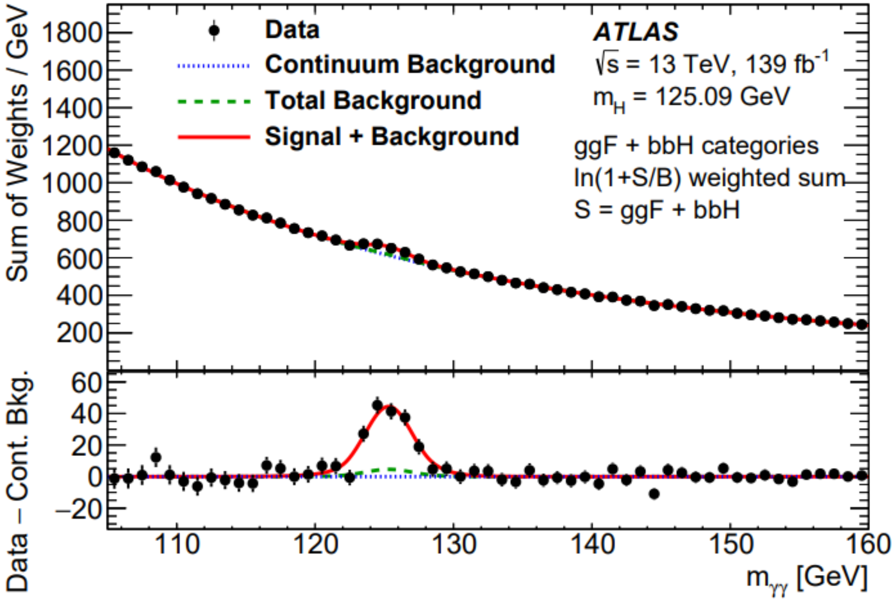

(a) ggF+ $b\bar{b}H$

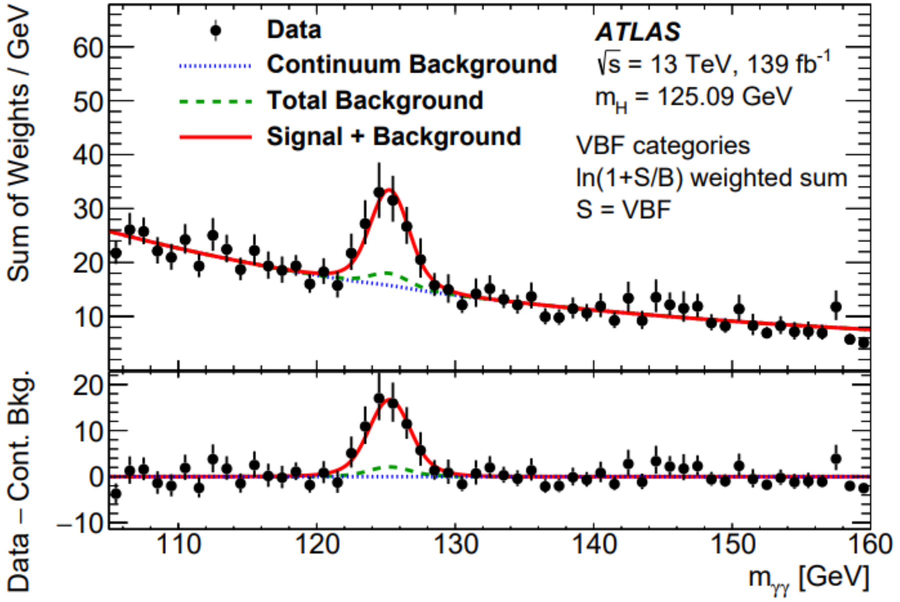

(b) VBF

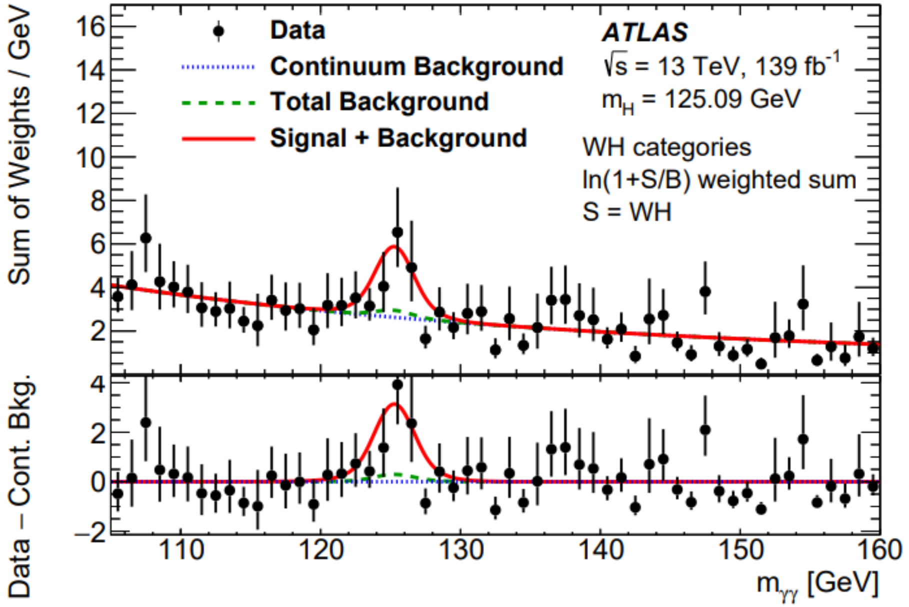

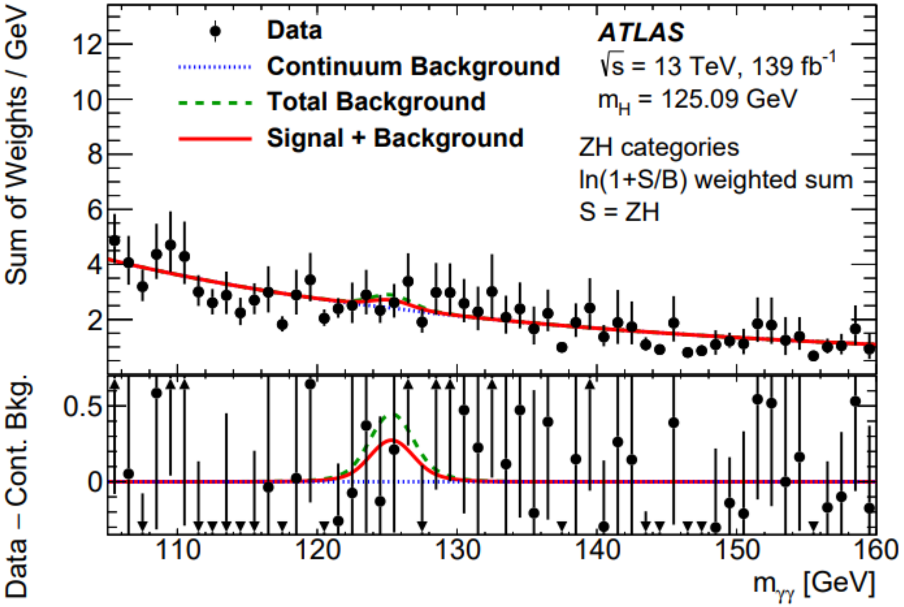

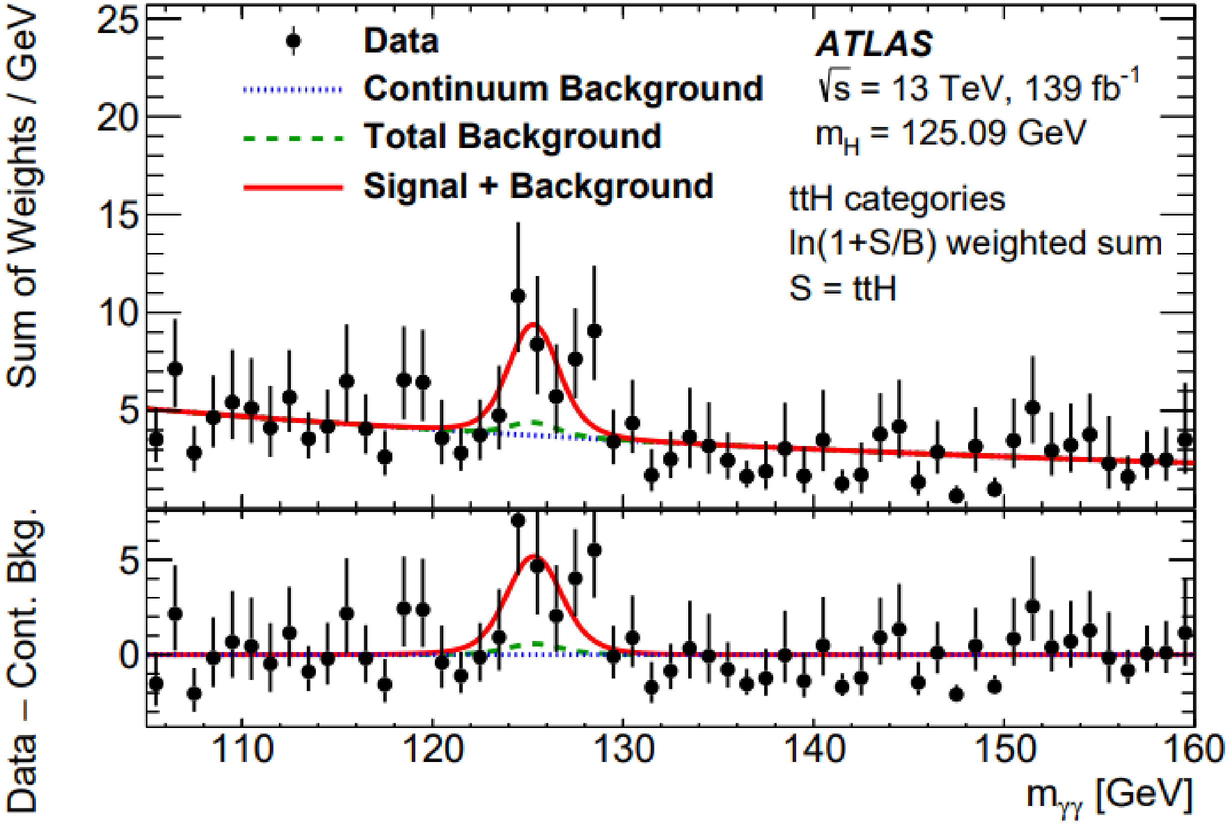
Sum of Weights / GeV
Data
Continuum Background
Total Background
Signal + Background
ATLAS
√s = 13 TeV, 139 fb-1
mH = 125.09 GeV
ttH categories
ln(1+S/B) weighted sum
S = ttH
25
20
15
10
5
Data − Cont. Bkg.
5
0
110
120
130
140
150
160
mγγ [GeV]

(e) $t\bar{t}H$

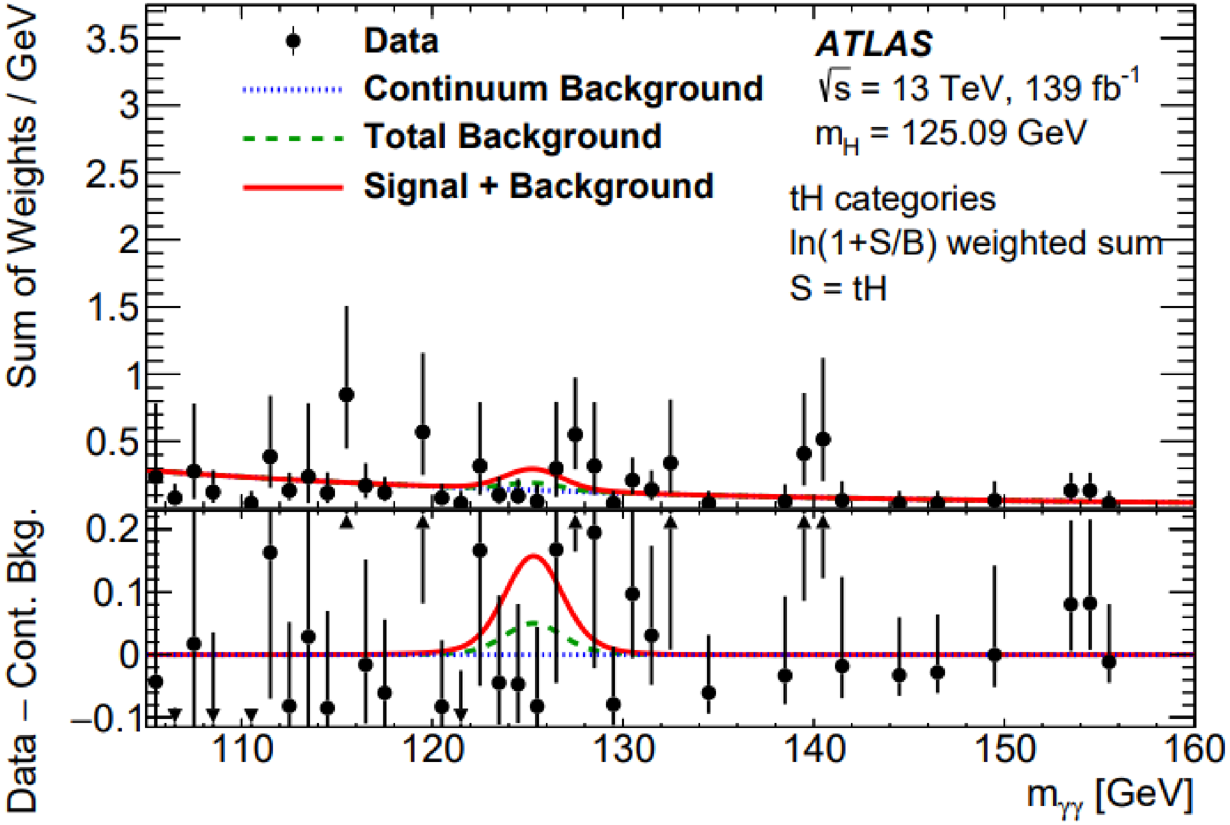
Sum of Weights / GeV
Data
Continuum Background
Total Background
Signal + Background
ATLAS
√s = 13 TeV, 139 fb-1
mH = 125.09 GeV
tH categories
ln(1+S/B) weighted sum
S = tH
3.5
3
2.5
2
1.5
1
0.5
Data − Cont. Bkg.
0.2
0.1
0
−0.1
110
120
130
140
150
160
mγγ [GeV]

(f) tH

From Michael Spira's slides

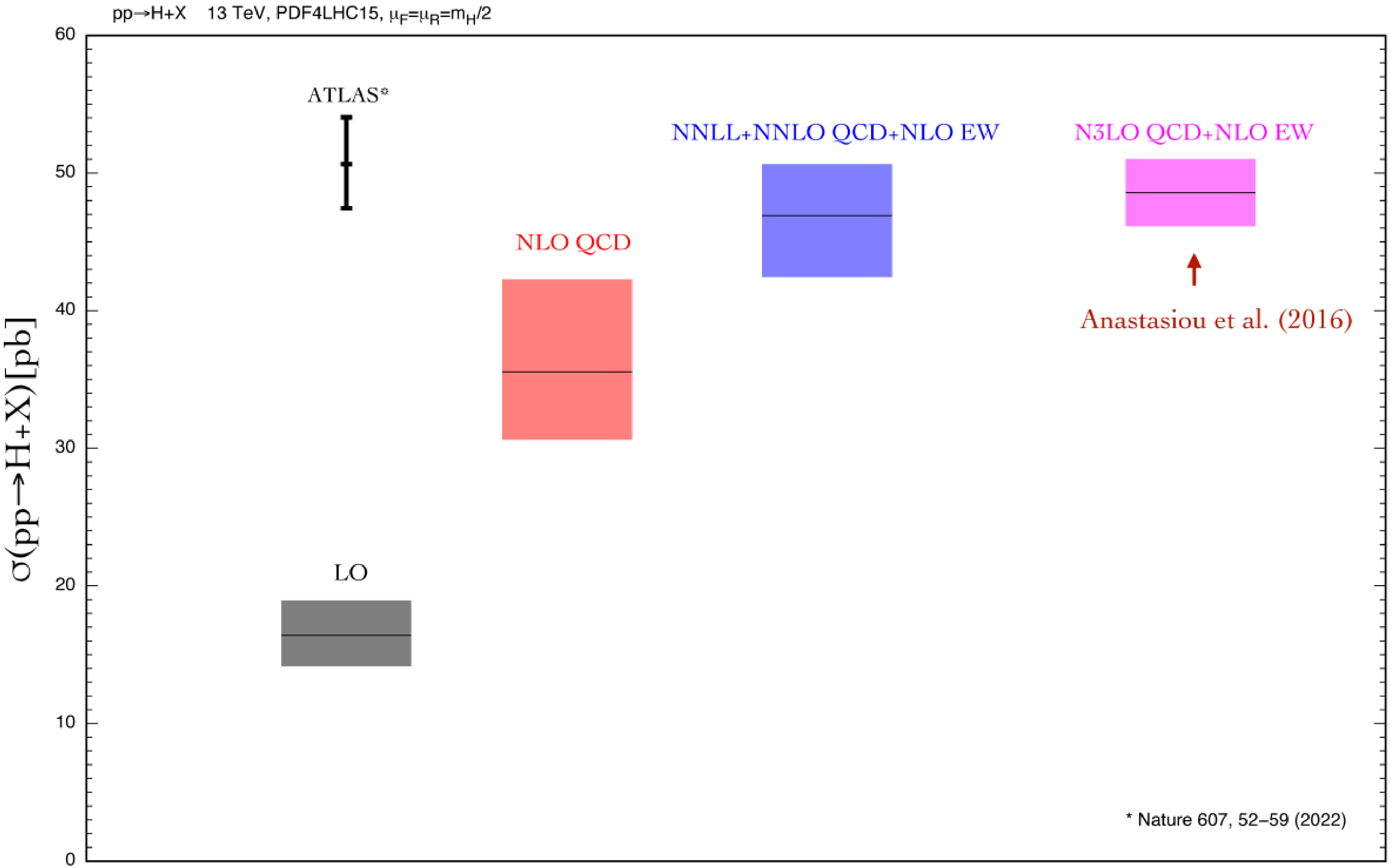

stolen from M. Grazzini@Higgs10

Interpretations of the measurements

- Signal strength

$$\mu \equiv \frac{\sigma_{observed}}{\sigma_{SM}}$$

- depends on reference, high syst error, evolves with knowledge of the SM

$$\sigma_{fiducial}$$

inclusive in production modes

Interpretations of the measurements

• Signal strength	$\mu \equiv \frac{\sigma_{observed}}{\sigma_{SM}}$	- depends on reference, high syst error, evolves with knowledge of the SM
• Cross-section	$\sigma_{fiducial}$	- specific for decay channel inclusive in production modes

Interpretations of the measurements

• Signal strength	$\mu \equiv \frac{\sigma_{observed}}{\sigma_{SM}}$	- depends on reference, high syst error, evolves with knowledge of the SM
• Cross-section	$\sigma_{fiducial}$	- specific for decay channel inclusive in production modes
• Differential cross-section	$\frac{d\sigma}{dX}, X = y, p_T, ...$	inclusive in production modes

Interpretations of the measurements

• Signal strength	$\mu \equiv \frac{\sigma_{observed}}{\sigma_{SM}}$	- depends on reference, high syst error, evolves with knowledge of the SM
• Cross-section	$\sigma_{fiducial}$	- specific for decay channel inclusive in production modes
• Differential cross-section	$\frac{d\sigma}{dX}, X = y, p_T, ...$	inclusive in production modes
• Kappa-framework	$\varkappa_i$	probes amplitudes (and interference) **specific to** a given **model (probes vertex)**

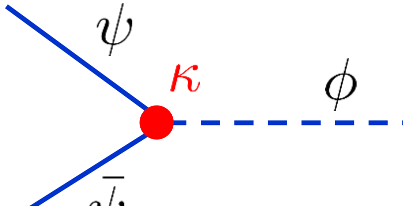

Higgs production and decay

Production modes

ggF

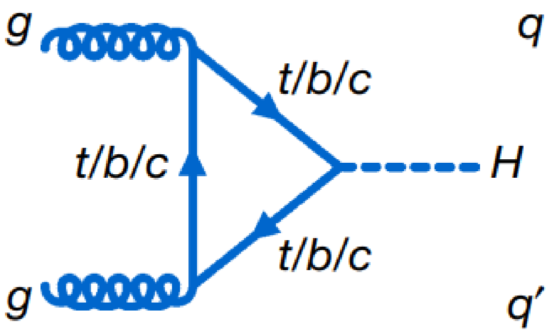

VBF

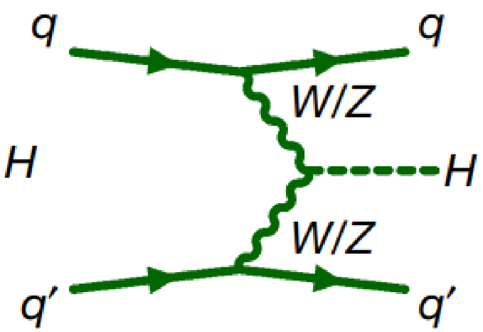

VH

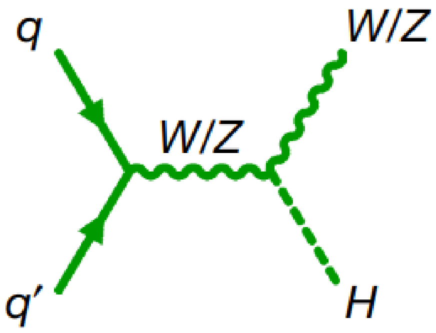

ttH

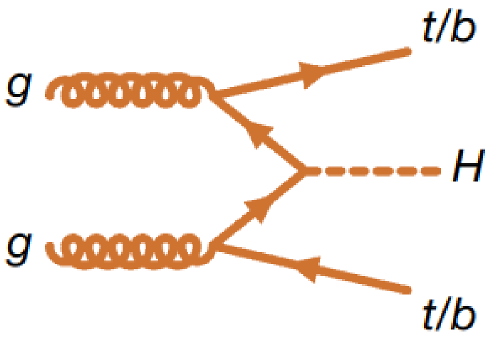

tHq

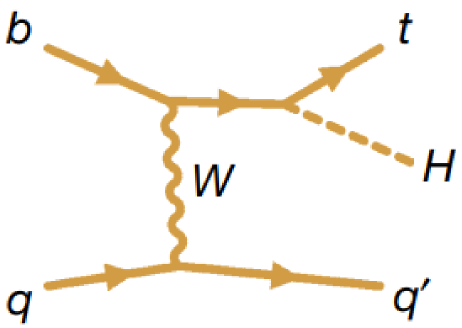

Decay channels

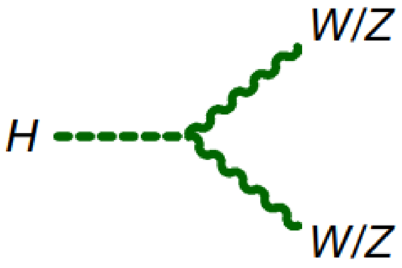

$H \longrightarrow \gamma\gamma$